WIND TUNNEL TESTS ON MODELS OF MERCHANT SHIPS

By K. D. A. SHEARER, D.R.T.C., and W. M. LYNN

12*th February*, 1960

SYNOPSIS.—*To provide accurate data on the wind resistance of certain modern ship designs, wind tunnel tests have been carried out on* 1/60*th scale models of a tanker and two cargo ships and on* 1/64*th scale and* 1/128*th scale models of a modern passenger liner.*

The tanker and cargo-vessel models were tested in three conditions of loading, and the magnitude and direction of the resultant force and moment about amidships for each complete model in the three conditions are given for a free stream tunnel velocity of 100*ft. per second over a range of relative wind from* 0 *to* 180 *deg. off the bow. These models were tested in a wind gradient.*

In the case of the modern passenger liner the larger model was tested in a wind-gradient condition and the smaller model in both the wind-gradient and uniform-wind conditions. The magnitude and direction of the resultant force and moment about amidships were measured. Two 1/128*th scale models were used for measuring the wind resistance in the uniform wind condition, one of them acting as a reflexion model.*

With the exception of the reflexion model all tests were carried out with the models in the boundary layer close to the tunnel roof. For the 1/64*th and* 1/60*th scale models the resultant velocity gradient was considered to be reasonably close to the gradient obtained under natural conditions above the surface of the sea.*

The model results are shown in a non-dimensional form using an ahead resistance coefficient K, and are compared with some published data.

Certain possible inaccuracies in applying the model results to the ship conditions are discussed. There are two appendices. The first considers the factors affecting the natural wind velocity gradient above the surface of the sea and the second gives results obtained from wind speed measurements made at various points on the models. Diagrams indicate possible serious errors in speed measurements due to poor siting of an anemometer.

Introduction

IN the last thirty years a certain amount of information has been published by different institutions and authorities on the wind resistance of various types of vessels. The most reliable series of experiments was carried out in the early part of this period and since that time there have been considerable changes in ship fashions and designs. Apart from differences in the proportions of vessels, modern superstructures tend to be more rounded and compact and the hull forms have greater sheer and flare of bow than previously.

Accurate information on the wind resistance of modern vessels has a number of applications including use in the analysis of measured-mile trials and voyage data, and for estimating mooring and towing forces.

In order to obtain this information wind-tunnel tests on certain typical modern superstructures and forms have been carried out in the Duplex Tunnel of the Aerodynamics Division of the National Physical Laboratory.

Many vessels spend a fair proportion of their services in the light and heavily trimmed conditions. Here the effect of wind forces may be most important and the programme of tests therefore included investigations into the wind resistance characteristics of the tanker and cargo-vessel forms in these conditions.

Choice of Ship Type

From a survey of contemporary oil-tanker and dry-cargo types involving the examination of the hull proportions, type and disposition of erections, etc., it was possible to obtain a broad indication of trends in the design of these vessels. It was desirable to test a design including the essential characteristics of each class without any excessive streamlining. Even within these limitations a large number of relatively minor variations was encountered and it was accepted that the model results might require some modification before application to an individual ship.

The oil-tanker form was based on the design of a 16,000-ton deadweight vessel.

On first examination the cargo vessels were split into two classes, i.e. those with two and those with three hatches on the upper deck forward of the bridge erection. It was considered that the position of the bridge erection relative to the forecastle or bow would be an important feature in the wind resistance characteristics of each type. A large proportion of the vessels under survey fell broadly within the two classes and subsequently two cargo ships were designed using a 10,000-ton deadweight vessel as a basic form.

The choice of the passenger vessel was determined by the existence of the models which had been constructed for other purposes. This vessel is fairly representative of recent designs for this type.

Particulars of Models

The models are designated :—

Model A	Oil Tanker
Model B	Cargo Vessel
Model C	Cargo Vessel
Model D	Passenger Liner

All models consisted of above-water hull and structure as shown in Fig. 28. Models B and C have two and three hatches forward of the bridge erection respectively and the scale of Models A, B and C was 1/60th full size.

For Ship D two models were built to 1/128th scale and one model to 1/64th scale. The scale of the latter model was determined by the existence of the larger model already constructed for other purposes. All three models had similar detailing of superstructure so that the results could be compared for models of different scale. The two small models were used for measuring the wind resistance in the uniform wind condition, one of the models acting as a reflexion model. This will be discussed later.

The principal dimensions and details of the conditions tested are given in Tables 1 and 2.

TABLE 1—*Principal Dimensions*

	Tanker A		*Cargo B & C*		*Passenger Liner D*		
					Model		
	Model	*Ship*	*Model*	*Ship*	*1/128th Scale*	*1/64th Scale*	*Ship*
Length, ft. Overall ..	9·27	556·0	8·13	488·0	6·28	12·56	804·0
B.P.	8·78	527·0	7·42	445·0	5·78	11·56	740·0
Beam ft.	1·21	72·5	1·03	61·79	0·76	1·52	97·0

TABLE 2—*Conditions Tested*

Condition	*Tanker A*		*Cargo B & C*		*Passenger Liner D*		
					Model		
	Model	*Ship*	*Model*	*Ship*	*1/128th Scale*	*1/64th Scale*	*Ship*
1. Deep loaded. Level trim							
Freeboard amidships ft.	0·13	7·75	0·21	12·67	0·29	0·58	36·75
Corresponding draught ft.	0·51	30·5	0·46	27·5	0·17	0·34	21·5
2. Light. (Approx. 60% load draught) level trim							
Freeboard amidships ft.	0·33	19·75	0·39	23·67			
Corresponding draught ft.	0·31	18·5	0·275	16·5			
3. Light. Large trim aft.	As condition 2, trimmed approx. 1 in 44 aft.						
Total trim over length bp ft.	0·20	12·0	0·167	10·0			

For the tanker and cargo vessel models, A1, A2, A3, B1, etc. will be used to indicate the various loading conditions. The model details and waterline relating to these conditions are shown in Figs. 1, 2 and 3.

All models were made of wood, smooth finished and given a coat of varnish. In the construction certain minor equipment was omitted such as wind-lasses, winches, bollards, fairleads and rigging. Rails and stanchions were only fitted where they were prominent as in the fore and aft gangway in the tanker form.

The two cargo ship models were designed with a common hull form to be used in conjunction with two sets of superstructures. The tanker model was made completely independent of this arrangement and had its own hull form. To enable tests to be carried out in the light and trim conditions two sets of wooden slabs were constructed for fitting to the base of each of the tanker and cargo forms. When the loaded condition was required the slab was removed leaving the model in the basic condition.

Photographs of models A1, B1 and C1 are shown in Fig. 28.

Experimental Procedure

It was desired to test the models in a wind velocity gradient similar to that existing in natural winds over the sea surface and the characteristics of the natural wind gradient over the sea are discussed in Appendix 1 with reference to published data on this subject. It was found that at a model scale of 1/60th or 1/64th the required gradient was reasonably close to the velocity profile existing at the roof of the wind tunnel working section. The models were therefore tested in this boundary layer by suspending them from the balance just clear of the tunnel roof.

Model C3 is shown in the testing position in Fig. 29. The tunnel boundary layer at the working section as determined by a pitot-tube traverse is shown in Fig. 4.

With regard to model D the conditions were not quite comparable for the different scale models since on increasing the scale a larger proportion of the model comes in to the uniform wind stream and the relative scales of the gradients are altered. The 1/128th scale model was also tested in the non-gradient or uniform wind condition using the reflexion model method. The arrangement for these tests is shown in Fig. 30, the lower model being the one on which the forces were measured.

The method of using an image model provides a plane of symmetry at the sea surface and even the thin boundary layer associated with a false floor is avoided. The " live " model was supported on guarded struts and the " image " model was clamped on to the strut guards.

Previous experience has shown that the relatively sharp edges present on ship models produce separated flow so that scale effects due to the change of state of the model boundary layer with Reynolds number are absent and forces and moments vary almost exactly with the square of the wind speed. Unfortunately, for separated flow the corrections to the measured resistance for the blockage of the model and its separated wake are larger and more uncertain than for models with attached boundary layers. Even so these corrections to the resistance of the 1/60th scale models only varied from about 3 per cent in the head-on condition to 15 per cent in the broadside condition. For the 1/64th model of the liner the blockage corrections would have exceeded 20 per cent for angles of yaw greater than 45 degrees and tests were restricted to angles up to 45 degrees.

Apart from blockage, there was a further small correction to resistance due to the action of the longitudinal pressure gradient in the wind tunnel on the models. For the large model of the liner this correction only amounted to six per cent and was independent of angle of yaw.

Model Results

The tanker and cargo vessel models were tested complete with superstructure in the three conditions of loading as previously described. Subsequently all superstructure above the continuous upper deck was removed and similar tests were carried out on the bare hulls.

All tests were carried out in a tunnel wind velocity of 61ft. per second in the free stream clear of the boundary layer, but for convenience the results have been corrected to a free stream tunnel velocity of 100ft. per second on the assumption that the forces vary as the square of the speed.

The diagram below indicates the forces measured.

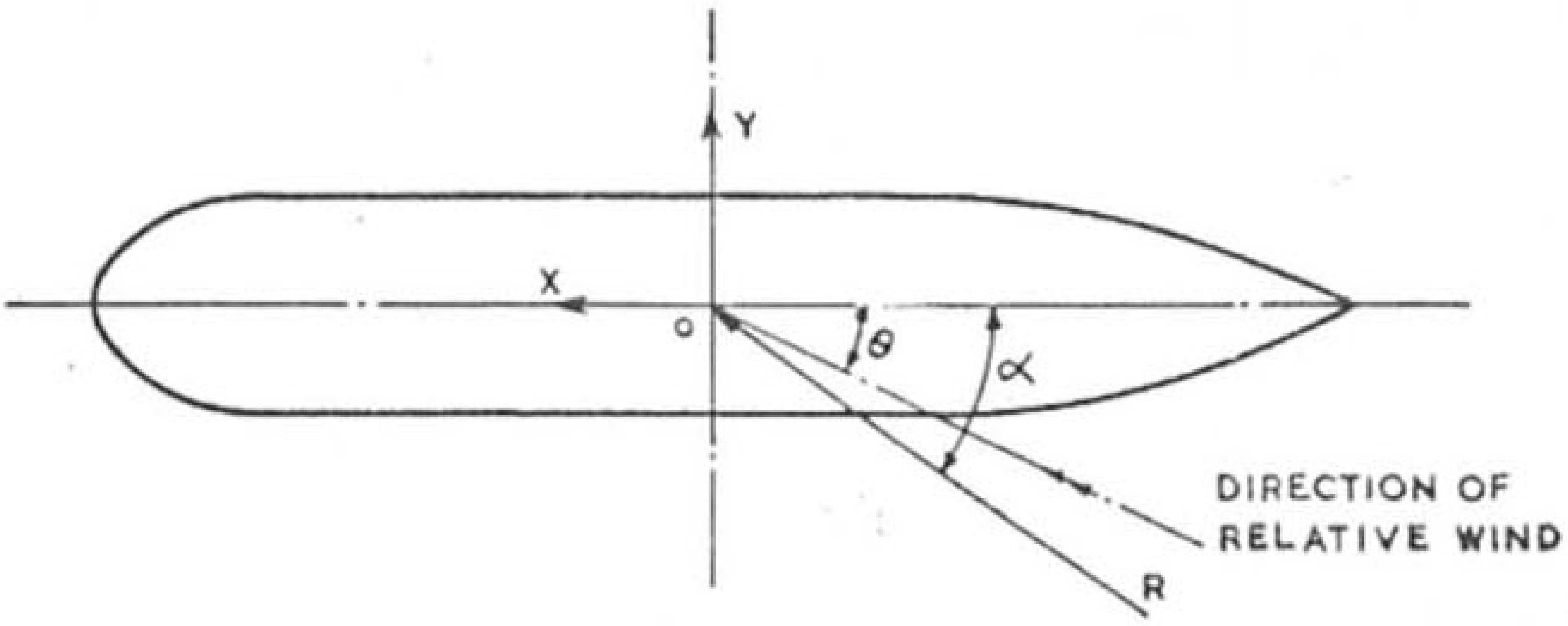

V_R = Relative wind speed, ft. per second.

V = Relative wind speed, knots.

θ = Direction of relative wind, deg.

N = Moment about amidships b.p., lb. ft.

X = Longitudinal force, lb.

Y = Lateral force, lb.

R = Resultant force $\frac{X}{\cos\alpha}$, lb.

α = Direction of resultant force, deg. = $\tan^{-1}\frac{Y}{X}$

The results are shown as follows :

Figs. 5, 6 and 7 — R and α values for the three conditions of loading for models, A, B and C and for bare hull tests where these were carried out.

Fig. 8 — R and α values for model D.

Figs. 9, 10 and 11 — N values for models A, B and C.

Fig. 12 — N values for model D.

Figs. 13 and 14 — $\frac{R}{V^2}$ values for full-scale ships A, B, C and D.

Figs. 15 and 16 — $\frac{N}{V^2}$ values for full-scale ships A, B, C and D.

On conclusion of the tests on the complete tanker model the hand rails and stanchions along the fore-and-aft gangway were removed and further tests carried out on the modified model. The test measurements relating to this condition, Model A2(a), are shown in Figs. 5 and 9. It will be noted that in general the effect of this removal is slight except where the original curve appears to be in error. It is considered that small details such as hand-rails on the model will have a relatively greater resistance effect than their full-size versions on the ship. The models were run in the bare-hull condition to obtain some indication of the contribution of the hull to the complete model resistance. The curves, however, must be treated with some care as the different hull conditions in the two cases, particularly at larger angles of relative wind off bow or stern, have the effect of exaggerating the true hull contribution.

The gradients appropriate to the large and small models of the passenger liner, Model D, are shown in Fig. 17. The gradient appropriate to the 1/60th scale Model A, B and C is not shown but lies very close to the 1/64th scale gradient.

With regard to the passenger-liner results shown in Fig. 8, the 1/64th model forces have been adjusted to the scale of the 1/128th model and to the appropriate gradient by varying the forces as the mean square of the velocities over the two gradients. A comparison of the results on this basis indicates reasonable agreement over the limited range and confirms the absence of any appreciable scale effect but having regard to the large blockage factors affecting the 1/64th model it was decided to place more reliance on the 1/128th model results.

These results were consequently adjusted to a gradient corresponding to the 1/64th scale using the relative mean square velocity of the two gradients to obtain the final condition.

Resistance Coefficients

For comparison with previously published data, the model results have been put in the form of two non-dimensional coefficients. These are :—

(i) Ahead resistance coefficient $= \dfrac{\text{ahead resistance}}{\frac{1}{2}\rho/g\ V_R^2\ A_T}$

(ii) Hughes's resistance coefficient

$$K = \frac{R\cos(\alpha - \theta)}{\rho/g\ V_R^2\ (A\sin^2\theta + C\cos^2\theta)}$$

where ahead resistance $= X = R\cos\alpha$; and X, R, θ and α have been defined earlier.

Also V_R = relative wind velocity, ft. per second.

A_T = transverse projected area, sq.ft.

A = longitudinal projected area, sq.ft.

C = equivalent transverse area

= $A\ (R_{\text{ahead}}/R_{\text{broadside}})$, sq.ft.

ρ = specific weight of air, lb. per cub. ft.

The value of ρ/g for the model tests was $0\cdot00237$ lb. sec.^{2}/ft.^{4} and for present purposes a free-stream tunnel wind speed of 100ft. per second has been used for V_R. The model areas are given in Table 3.

Ahead Resistance Coefficient

The ahead resistance coefficients for the three conditions of loading of Models A, B and C over the complete range of direction of relative wind are given in Figs. 20, 21 and 22. The coefficients for Model D are given in Fig. 23. These coefficients can be used directly to obtain the wind resistance of the full-scale counterparts of the various models using the free stream relative wind speed V_R clear of interference.

It may be desirable to use the coefficients to obtain an indication of the wind resistance of much smaller vessels of similar types to those tested. In these cases owing to their low freeboard the vessels will be operating only in the lower portion of the wind-gradient curve and the resistances would be appreciably less than those indicated from the present results.

Hughes's Resistance Coefficient

The resistance coefficient K was introduced by Hughes and uses the artificial area term C so that the value of the coefficient for $\theta = 0$ deg. will be the same as for $\theta = 90$ deg. when K becomes the broadside coefficient $R_{\text{broadside}}/\rho/g\ AV_R2$. The value of the coefficient at 90 degrees is important and is approximately the same for experiments carried out in similar conditions and decreases with the introduction of the wind gradient. This is shown in Fig. 19 where the values obtained from various tests lie in order of severity of wind gradient.

TABLE 3—*Model Areas*

	Tanker A			*Cargo B*			*Cargo C*			*Passenger liner*	
	1	2	3	1	2	3	1	2	3	1/128*th* *model*	1/64*th* *scale model*
Transverse projected area (A_T) sq.ft.	0·903	1·144	1·144	0·826	1·015	1·015	0·808	0·997	0·997	0·64	2·56
Longitudinal projected area (A) sq.ft.	3·467	5·209	5·209	3·475	4·831	4·831	3·503	4·859	4·859	3·41	13·64
Equivalent transverse area (C) sq.ft.	1·236	1·240	1·315	0·843	0·859	0·872	0·856	0·834	0·846	0·385	1·54

The additional curves shown in this figure were obtained from the published results of tests on models of the following vessels :—

(a) *San Gerardo*[1]	Tanker in light level-keel condition.
(b) *London Mariner*[1]	Cargo vessel in loaded level-keel condition.
(c) *Liberty* vessel[2]	Cargo vessel in extreme light condition with 5ft. total trim aft.
(d) *Mauretania*[1]	Passenger liner.

In studying the various results it is important to consider the different experimental methods employed. Thus (a), (b) and (d) were tested using inverted models towed through water in an experiment tank while (c) was tested in a wind tunnel with a wind gradient, the forces being measured by electrical strain gauges.

In the case of (c) the model did not include some of the minor structure and equipment. The overall accuracy of these data is probably lower than in the present series of wind-tunnel tests. With the experiments carried out in water the accuracy is likely to be lower at the larger angles of yaw where wave-making occurs at very low speeds of advance.

Fig. 21 gives a comparison of the velocity gradients relating to the present series of tests and to the model of the *Liberty* vessel.

For models A, B and C the effect of changing from a wind gradient to a uniform wind is greatest in the case of the deeply loaded vessels with small free board, where the Hughes broadside resistance coefficient obtained for tank or wind-tunnel tests in uniform wind is 0·60. Thus the effect of the wind gradient is to reduce the resultant force at 90 degrees by up to 45 per cent. For model D in the 1/64th gradient the corresponding figure is approximately 30 per cent.

Basic Air Resistance

For models A, B and C it is possible to obtain a reasonably accurate estimate of the effect of the wind gradient when θ equals 0 degrees by using the bare hull and complete model results. It is found that to obtain the basic air resistance, i.e. the resistance in the absence of any true wind, it is necessary to add about 25 per cent to the value of the ahead-resistance coefficient in the light condition and 40 per cent in the loaded condition.

For model D the coefficient can be obtained directly from the results in the uniform-wind condition and the corresponding addition to the ahead-resistance coefficient is 21 per cent.

The above corrections have been obtained by using the height of the models from the waterline to the top of the bridge. It is possible that an effective height less than this should be assumed in which case the corrections would be increased.

Yawing Moments

Figs. 9, 10, 11 and 12 give the moments about amidships b.p. for models A, B and C in the various conditions of loading and model D. The yawing moment is equal to the product of the lateral force and the distance from centre of pressure to centre of lateral resistance of the underwater body and for present purposes the latter has been assumed to lie at amidships.

General Considerations

It is appreciated that the method of adjustment from one gradient to another (or to the uniform wind condition) using the mean square velocity over the respective gradients is an approximation. If the measured resistance obtained from tests in the 1/128th gradient is corrected by the mean square velocity method to that appropriate to uniform wind conditions, good agreement is obtained with the resistance measured in the tests in uniform wind at yaw angles up to 30 degrees. Above 30 degrees the resistance was, however, underestimated by up to 35 per cent. This difference would be appreciably less for the relatively small adjustment between the 1/128th and 1/64th gradients.

With regard to scale effect, previous work has indicated that owing to the sharp edges and irregular nature of a ship's hull and superstructure it should not be necessary to make any correction when applying results of model wind-resistance tests to the ship. This conclusion has been confirmed within reasonable limits by the results from the two sizes of model D and by full-scale tests as carried out, for example, on the *Lucy Ashton*. Certain cylindrical items such as masts and derrick posts will be affected, however, and will have higher resistance coefficients on the model scale than on the full scale. In cargo vessels with relatively large numbers of masts and derrick posts any error due to scale effect on these items is usually more than compensated by the additional resistance of the wire rigging which becomes appreciable in such circumstances.

The difficulties of simulating in model experiments the actual conditions of a ship advancing into a natural wind are considerable and it is fully appreciated that the present tests do not fulfil all the requirements. The results of wind-tunnel model tests carried out in a wind gradient are only directly applicable to natural winds blowing over stationary or moored vessels. When a vessel is advancing in a natural wind it is evident that the wind effect will be due to a combination of the natural true wind which has a velocity gradient and the wind created by the ship's own motion which is of uniform velocity. There will, therefore, be a mean velocity gradient which will vary according to the relative speeds of the vessel and the wind.

As mentioned earlier, it was considered that in applying the model results to the condition of the vessel advancing in calm air the ship's ahead resistance would be underestimated in the case of the tanker and cargo vessels in the light conditions by about 25 per cent and in the case of the passenger liner by about 21 per cent. This difference would be reduced by more than half for the case of a true wind dead ahead equal to the ship's speed, and the difference would continue to reduce as the true wind speed increased relative to that of the ship's speed.

Acknowledgments

The authors wish to thank the Council of the British Shipbuilding Research Association and the Director of Research for permission to publish this paper. They are also indebted to the staff of the Aerodynamics Division, of the National Physical Laboratory who carried out the tests on behalf of the Association. The results of these tests are given in the following N.P.L. reports to B.S.R.A.:—

1. Wind Resistance Tests on Three Cargo Vessels for B.S.R.A. (D. H. Williams, H. L. Nixon and W. C. Skelton) 1953.
2. Wind Resistance Tests on Models of a Modern Passenger Liner for B.S.R.A. (W. G. Raymer, H. L. Nixon) 1957.

REFERENCES

1. Hughes, G., " The Air Resistance of Ship's Hulls with Various Types and Distributions of Superstructure," *Inst. E. & S. in Scot.*, **75**, (1932), p. 302.

1a. Hughes, G., " Model Experiments on the Wind Resistance of Ships," *R.I.N.A.*, **72** (1930), p. 310.

2. Long, M. E., " Wind-Tunnel Tests on Multiple Ship Moorings. Part 3," *David W. Taylor Model Basin Report No.* 839, 1952.

3. Deacon, E. L., " Vertical Profiles of Mean Wind Velocity in the Surface Layers of the Atmosphere," *Chemical Defence Experimental Station, Porton*, Technical Paper No. 39, 1948.

APPENDIX 1

Many investigations of the behaviour of natural winds blowing over land and sea have confirmed the existence of a velocity gradient in the lower layers of the atmosphere. Probably owing to the difficulties in obtaining accurate measurements above the open sea the great majority of the data refer to the behaviour of the wind above various land surfaces and data relating to conditions above the sea are comparatively scanty.

The results which have been published show some disagreement but in Fig. 17 a typical curve of the wind-velocity gradient over the sea as derived from actual measurements is shown, together with another curve relating to the velocity gradient above a surface of smooth snow.

It is evident that the velocity gradient can be influenced by the surface roughness of the sea, but in a paper by Deacon[3], which summarizes some of the more reliable data it is concluded that the roughness effect is actually less than that indicated by some of the results and for moderate or fresh winds is more or less independent of wind velocity.

The velocity gradient is also influenced by the relative temperature at different levels in the atmosphere, i.e. the temperature gradient. The curves shown in Fig. 17 relating to velocity gradient above the sea and a surface of smooth snow apply to the condition without temperature gradient. Where the temperature increases with increase in height above the surface level, the velocity gradient tends to decrease more slowly than under constant-temperature conditions and the effect can be appreciable when the temperature variation is large. The tendency would be reversed but to a lesser extent with a decrease in air temperature upwards.

APPENDIX II—*Wind-velocity Measurements*

In the course of the wind-resistance tests on models A, B and C described in the paper, certain wind-velocity measurements were obtained at various positions above the vessel's superstructure. By this means the model experiments could be related directly to the full-scale ship conditions, as in the ship the wind speed would be measured by hand or recording anemometer at one of these positions.

The model speed measurements were made with a type of Booth tube consisting of two fine tubes welded together, with holes on the windward and leeward side of the instrument. The tube was rotated so that it always faced the relative wind and was kept in the same position on each model as the model was turned in different directions. It was known that the speed measurements were liable to error if the flow at the point of observation deviated markedly from the direction of the relative wind, and for this reason observations were made with streamers over the forward part of one model and over the bridge structure. It was found that the direction did not vary more than 5 deg. from the tunnel axis at the points chosen.

The wind-speed observations on the three models in the various conditions were obtained simultaneously with the wind-resistance measurements and principally at various levels on the centre line above the wheel-house at the forward end of the bridge erection. In the Cargo C model, this position was in way of an iron beam across the tunnel and an alternative position slightly forward was accepted.

The various positions at which the wind speeds were measured are indicated in Figs. 1, 2 and 3. The measurements were obtained for all complete models at heights equivalent to 6, 15 and 25ft. above the wheel-house top. The approximate heights above the waterline for the various ships and loading conditions are given in Table 4 for the 15-ft. position.

TABLE 4

	Tanker A			*Cargo B*			*Cargo C*		
	1	2	3	1	2	3	1	2	3
Height of 15-ft. position above water-line, ft.	57	69	71	60	71	71	60	71	63

As an indication of the effect of the model interference on the wind flow, the wind speeds measured at the various points have been expressed as ratios of the velocity in free flow.

The results are shown as wind "roses" in the following diagrams :—

Fig.	*Model*	*Level above wheel-house top, ft.*
24	A2	6, 15 and 25
25	C2	6, 15 and 25
26	A2, B2 and C2	15
27	B2 (complete and bare hull)	15

As might be expected in view of the similarity between the two main bridge structures, the wind roses for Models A and B were very much alike and thus the diagram for B2 at the various heights has not been included.

Whereas, as shown in Figs. 24 and 25, there are distinct differences in the wind-speed characteristics of Models A2 and C2 at the 6-ft. position, there is little difference between the models at the 15-ft. level and changes of condition and trim within the experimental limits have no appreciable effect (Fig. 26).

The local dip in the curves, particularly of Models B and C, between 0 and 5 degrees of relative wind direction off the bow, is due to interference of the masts and derricks immediately forward of the bridge.

Fig. 27 is of particular interest as it shows the wind speeds measured at the same point 15ft. above the wheel-house of Model B2, for the complete model and for the bare hull, i.e. after removing all superstructure above the continuous upper deck. The two curves are very similar except for the portion close to the centre-line where the masts on the complete model cause a local interference. From this it would appear that at the 15-ft. level above the wheel-house top (i.e. approx. 70ft. above the waterline) the principal interference is due to the ship's hull and the local disturbances due to shape of bridge, break of fo'c'sle, etc., which are important at the 6-ft. level, are no longer effective.

In conclusion it is considered that these measurements obtained on the 1/60th-scale models could be used to correct the wind speeds measured on the full-size vessels. This applies particularly to the curves relating to the 15-ft. and 25-ft. levels, but the curves for the lowest level must be used with care as they are clearly sensitive to small differences in the bridge structure.

The curves indicate the very serious errors that can result from the use of a hand anemometer at the 6-ft. level, in certain conditions only 25 per cent of the free wind speed being recorded. At the 15-ft. position, the measurements are more satisfactory except for relative winds at small angles ahead and astern. Apart from this, however, the measurements obtained over a considerable arc would probably be high to the extent of about 10 per cent. From these results it is clearly impracticable to improve on this performance except by raising considerably the level of the anemometer.

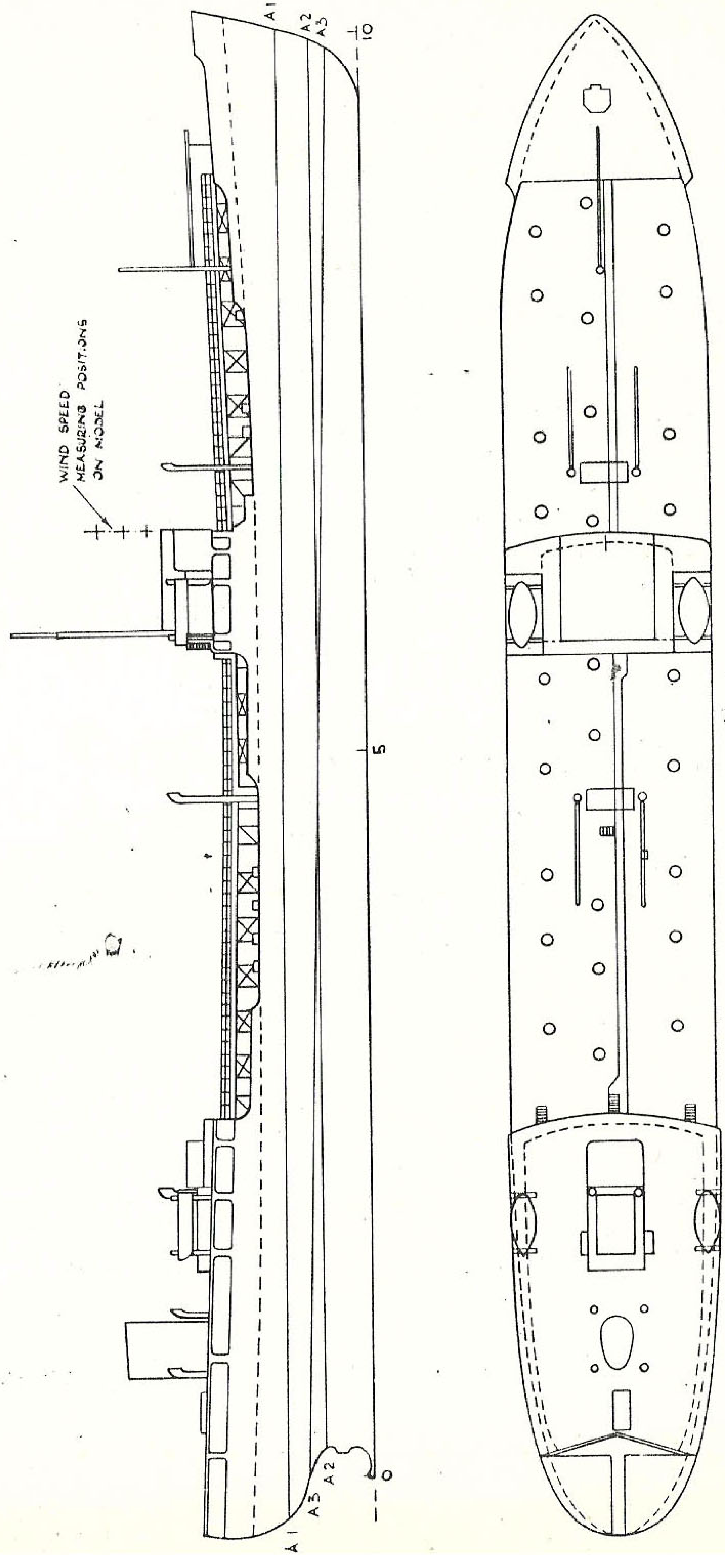

Fig. 1—Tanker "A"

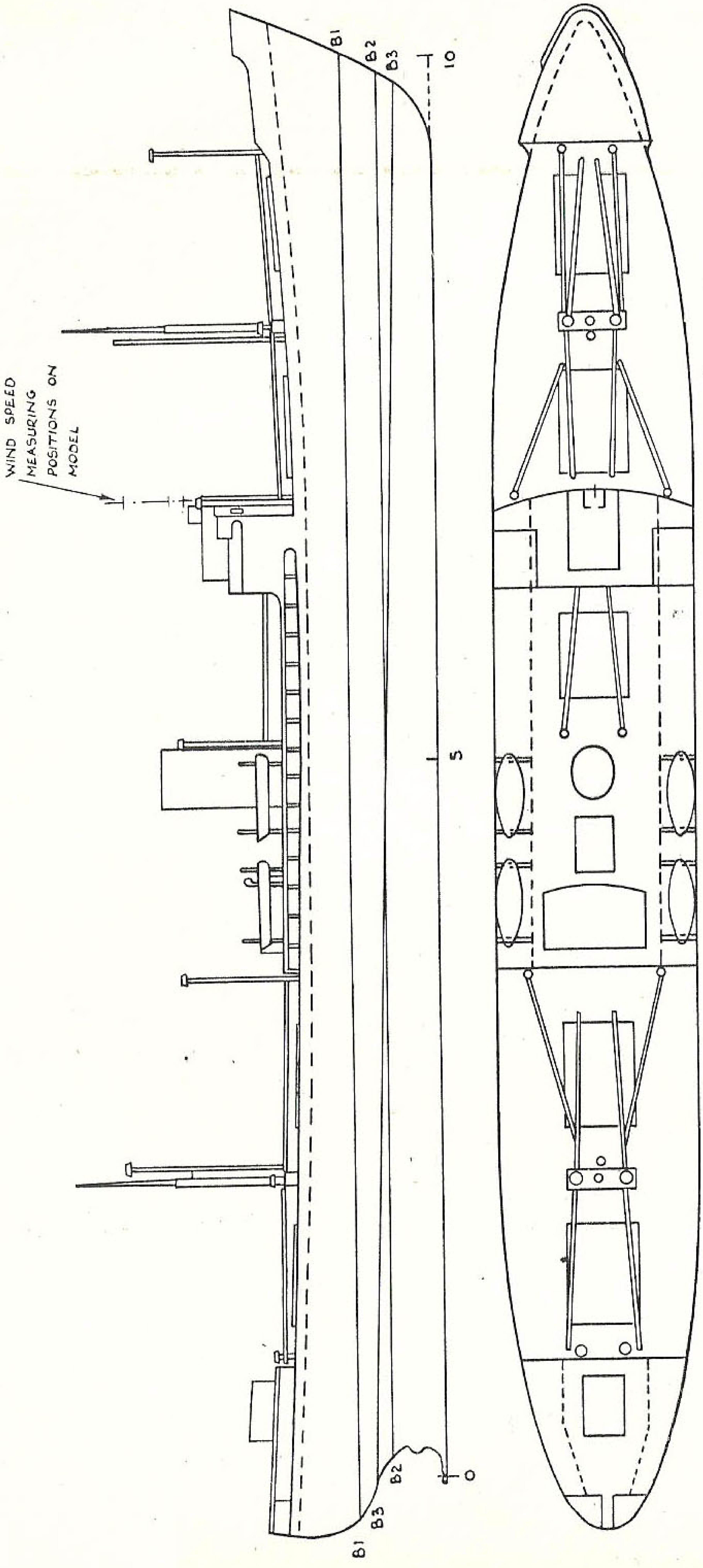

Fig. 2—Cargo " B "

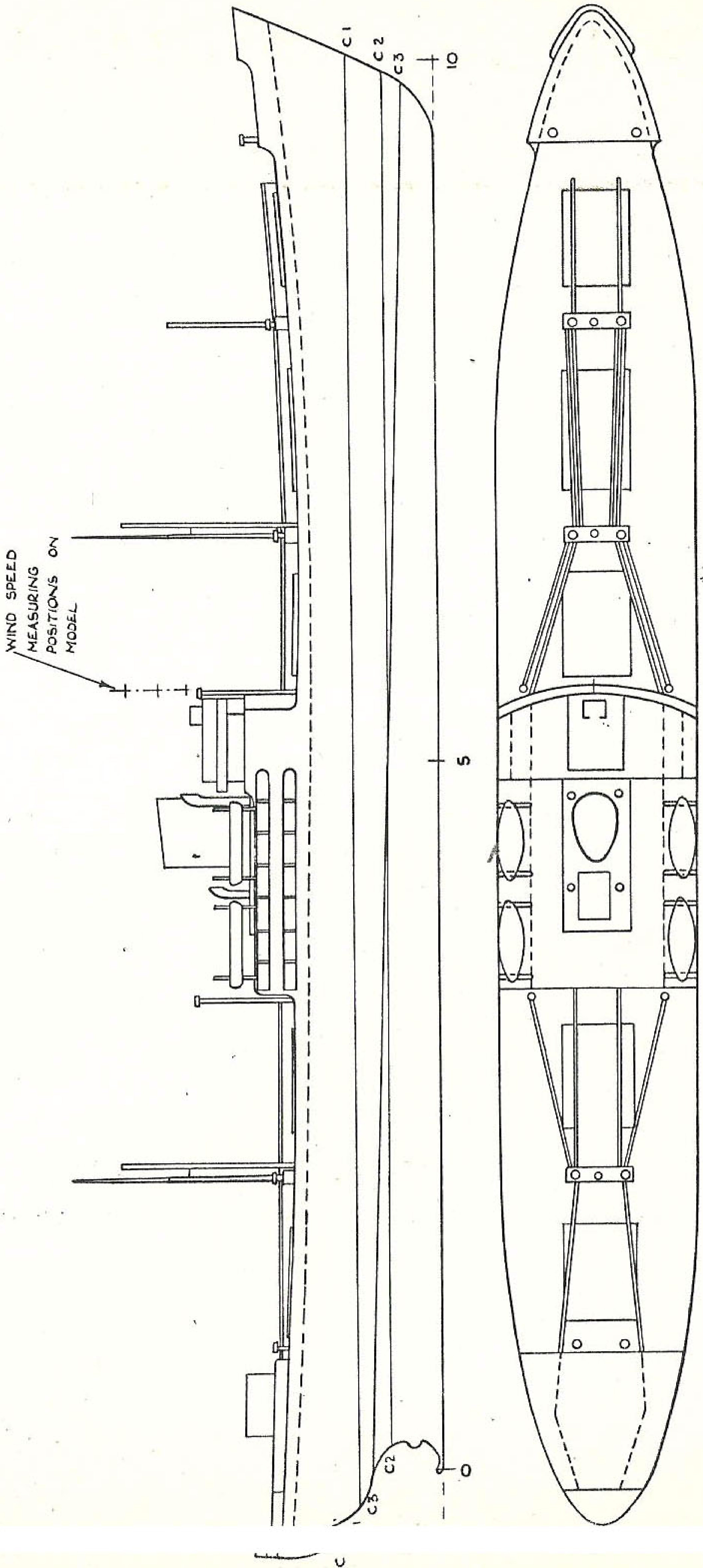

Fig. 3—Cargo "C"

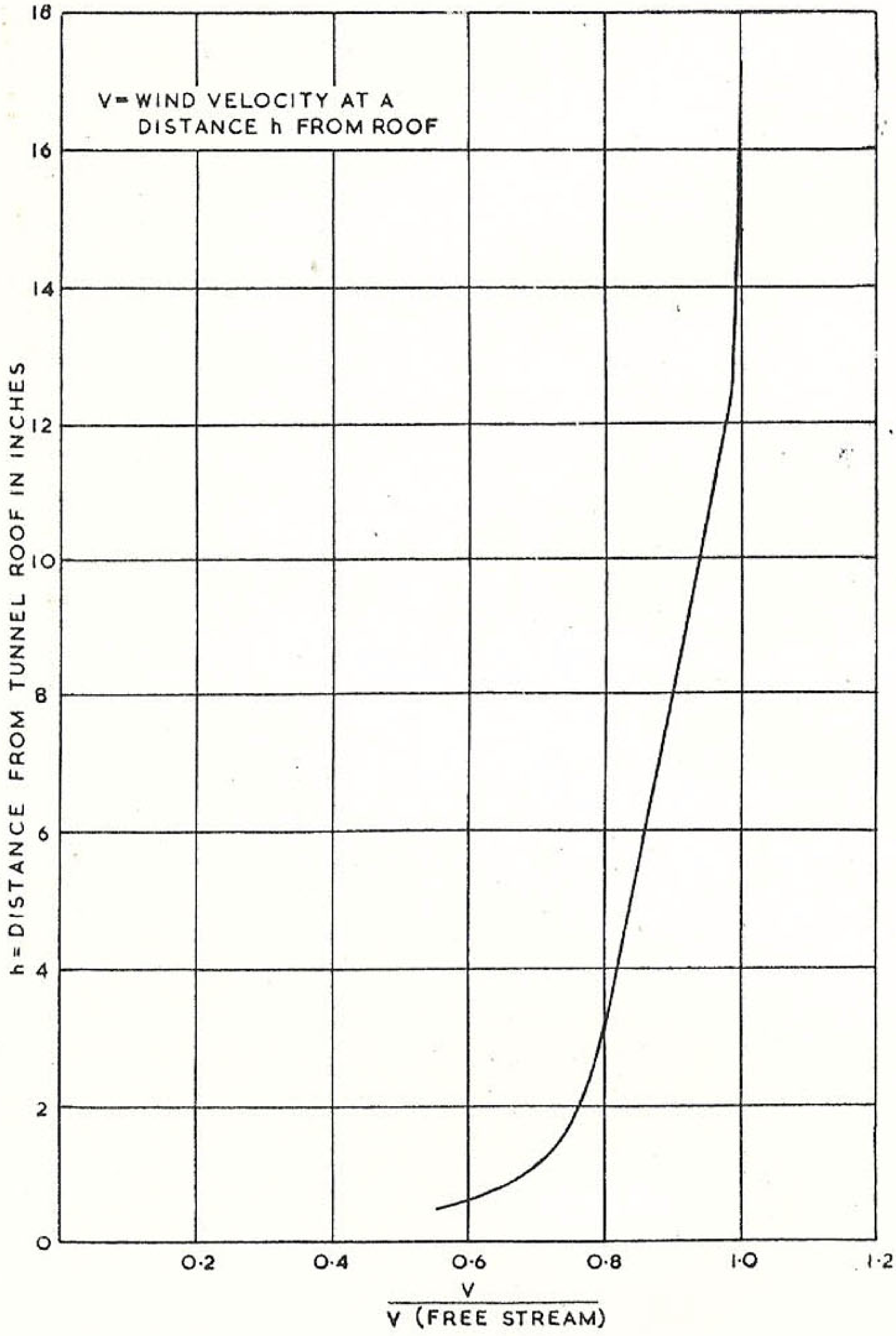

Fig. 4—Tunnel Wind Velocity Gradient determined by Pitot Traverse from Tunnel Roof Down Towards Centre at Working Section

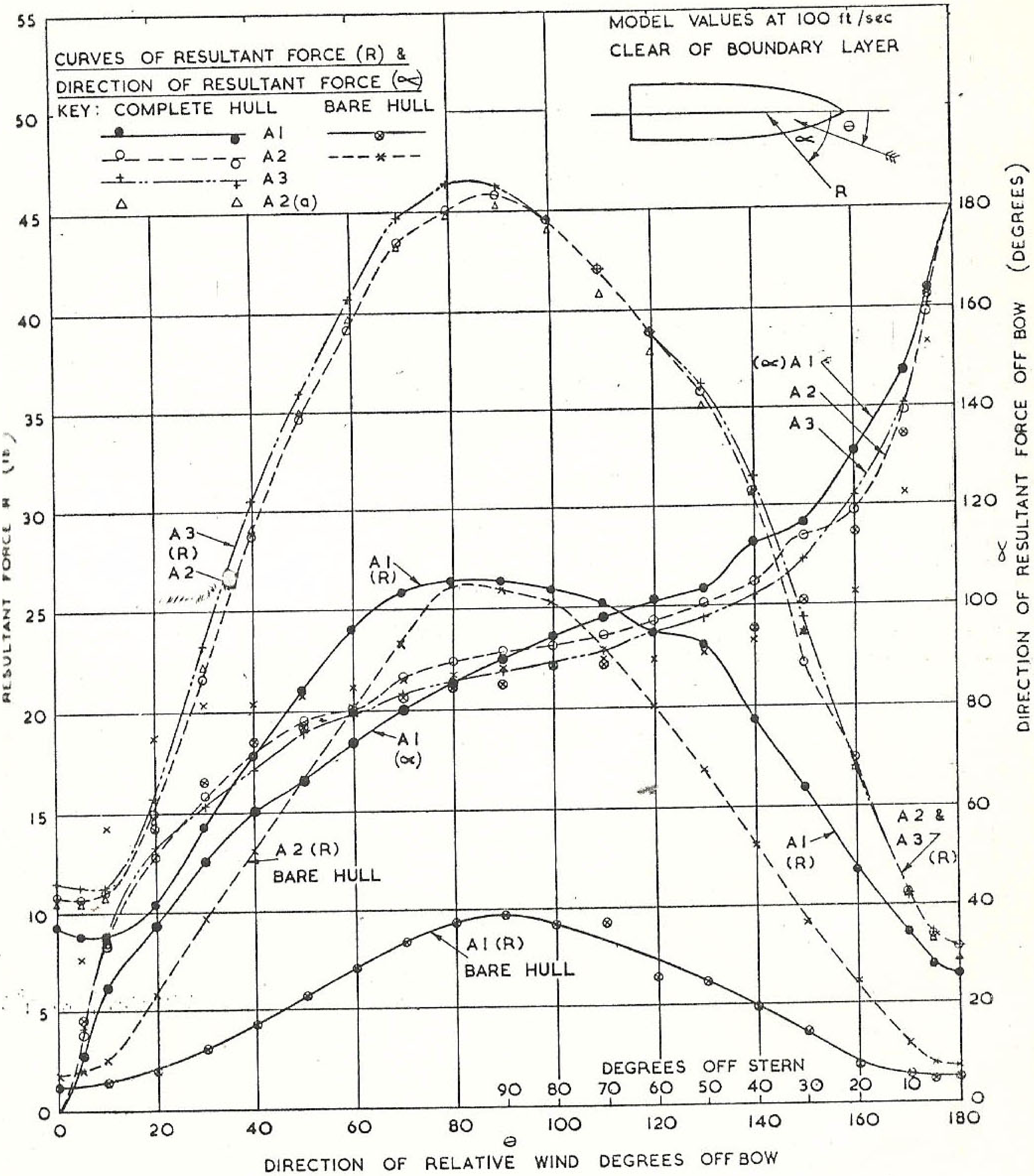

Fig. 5—Tanker " A "

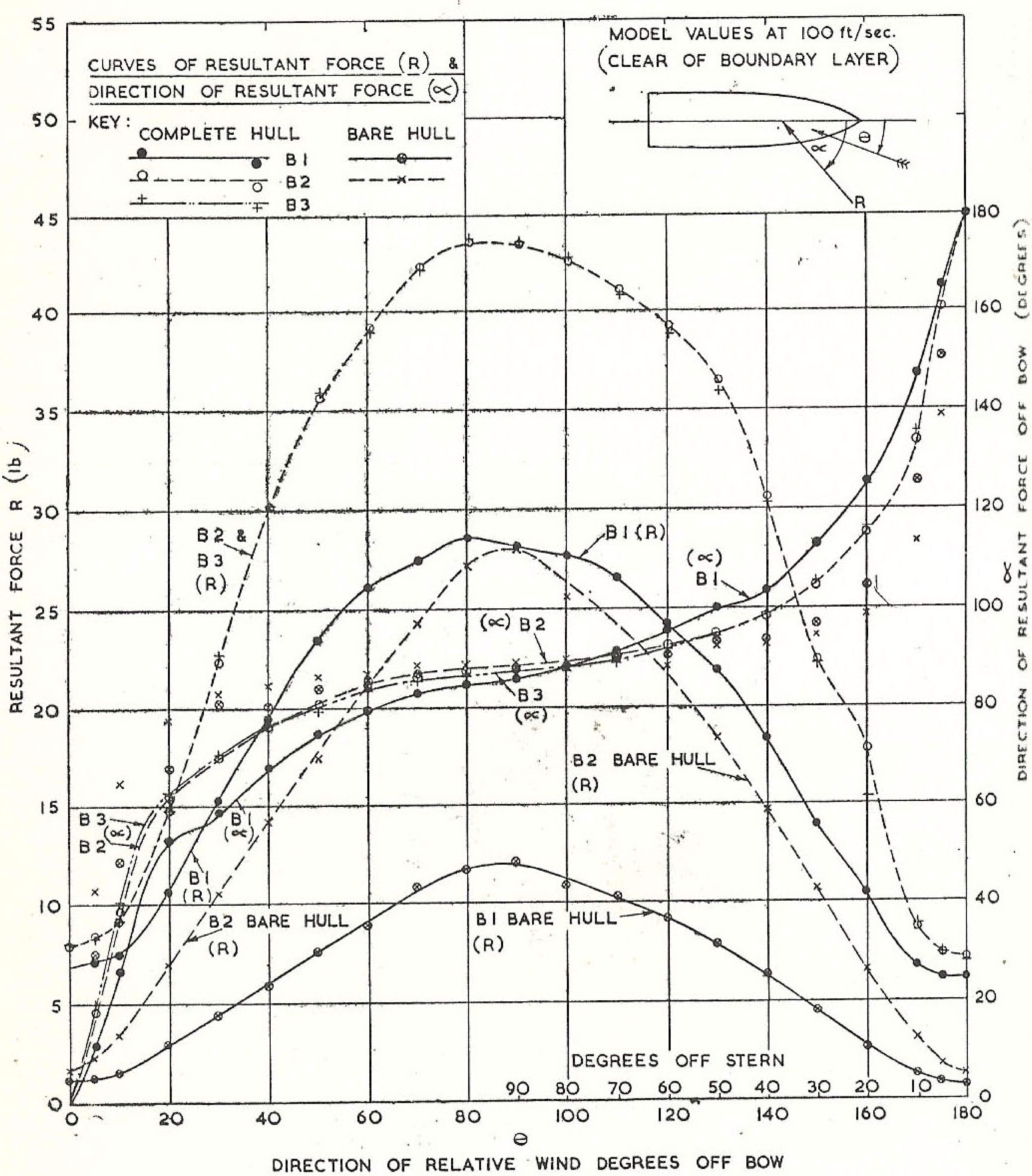
CURVES OF RESULTANT FORCE (R) & DIRECTION OF RESULTANT FORCE (∝)
KEY: COMPLETE HULL BARE HULL
B1
B2
B3
MODEL VALUES AT 100 ft/sec. (CLEAR OF BOUNDARY LAYER)
R
∝
θ
B2 & B3 (R)
B1 (R)
(∝) B1
(∝) B2
B3 (∝)
B2 BARE HULL (R)
B1 BARE HULL (R)
B3 (∝) B2
B1 (∝)
DEGREES OFF STERN
RESULTANT FORCE R (lb)
DIRECTION OF RESULTANT FORCE OFF BOW (DEGREES) ∝
θ
DIRECTION OF RELATIVE WIND DEGREES OFF BOW

Fig. 6—Cargo " B "

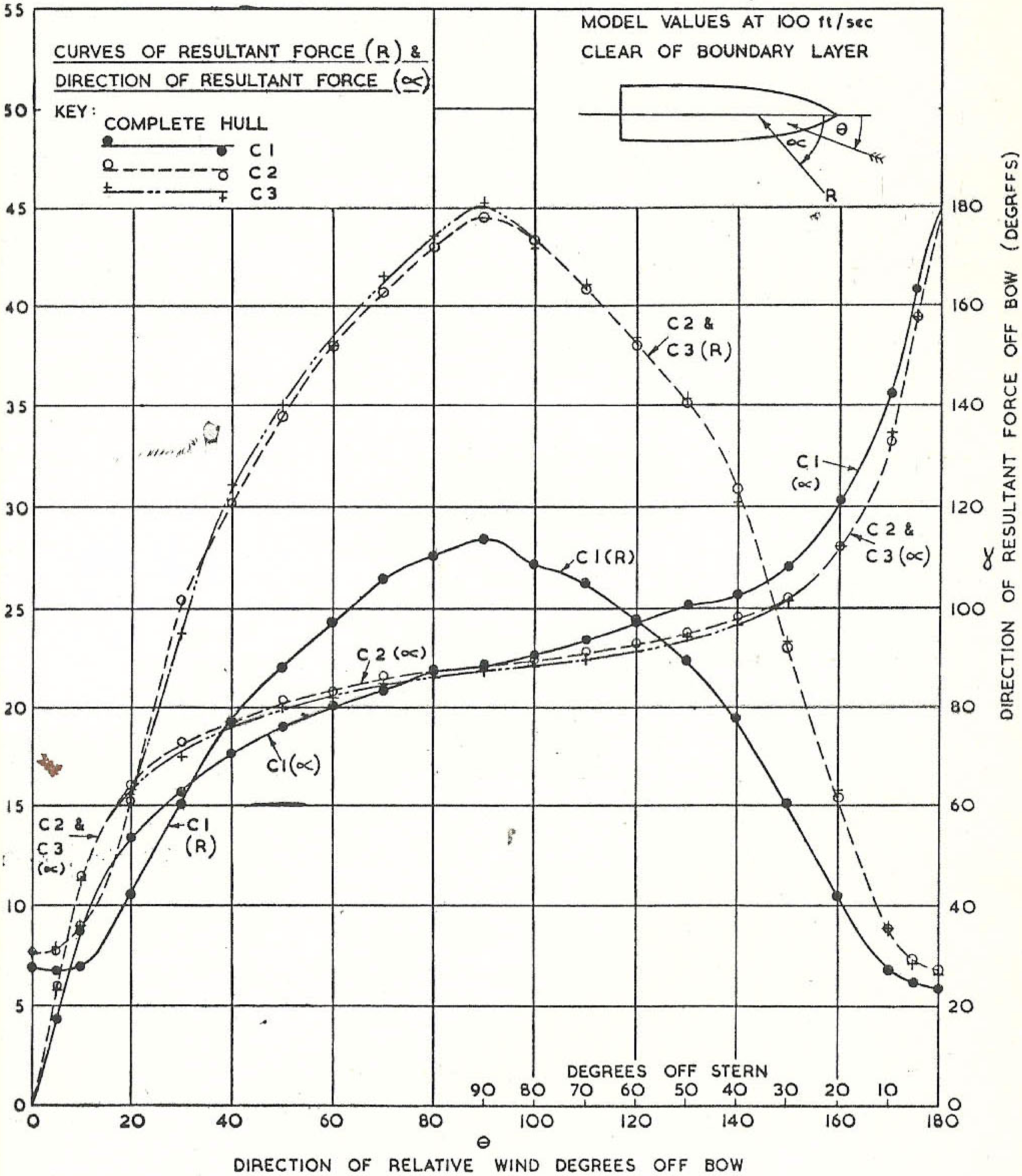
CURVES OF RESULTANT FORCE (R) &
DIRECTION OF RESULTANT FORCE (∝)
KEY:
COMPLETE HULL
C 1
C 2
C 3
MODEL VALUES AT 100 ft/sec
CLEAR OF BOUNDARY LAYER
θ
∝
R
C 2 & C 3 (R)
C 1 (∝)
C 2 & C 3 (∝)
C 1 (R)
C 2 (∝)
C 1 (∝)
C 2 & C 3 (∝)
C 1 (R)
DEGREES OFF STERN
90 80 70 60 50 40 30 20 10
0 20 40 60 80 100 120 140 160 180
0 5 10 15 20 25 30 35 40 45 50 55
0 20 40 60 80 100 120 140 160 180
θ
DIRECTION OF RELATIVE WIND DEGREES OFF BOW
∝
DIRECTION OF RESULTANT FORCE OFF BOW (DEGREES)

Fig. 7—Cargo "C"

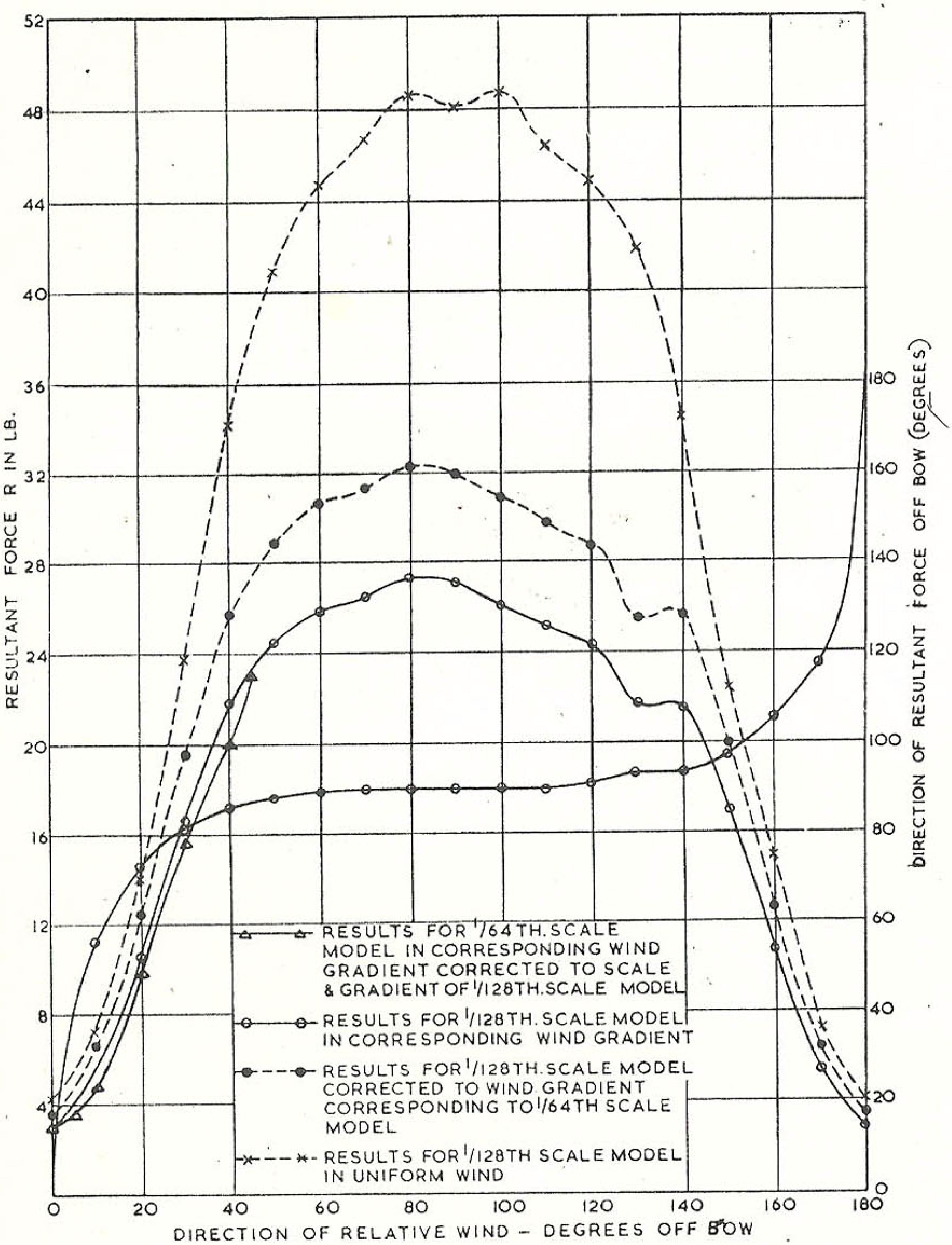

Fig. 8—Curves of Resultant Force for Model D (for Wind Velocity of 100ft. per sec.)

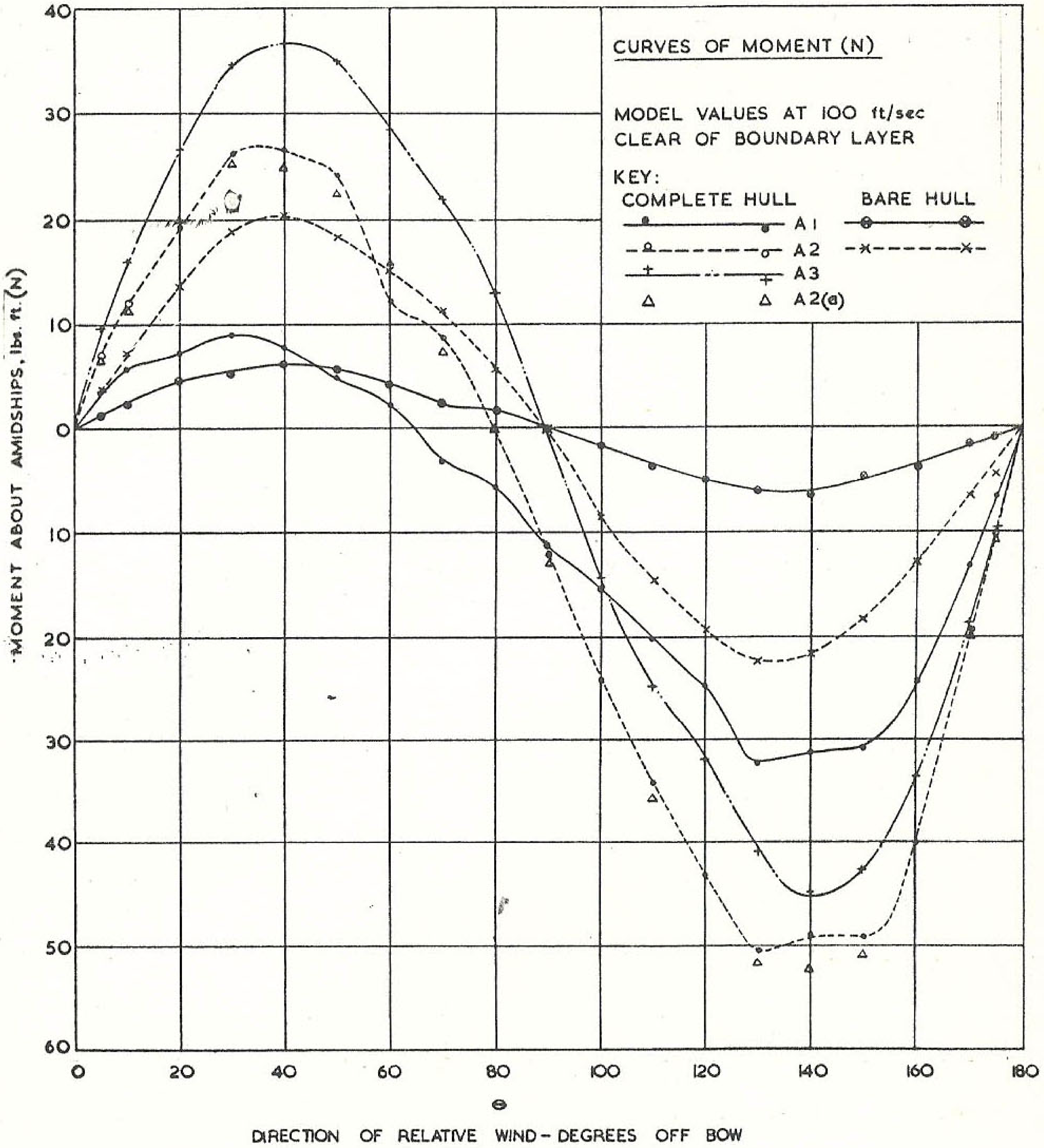

Fig. 9—Tanker "A"

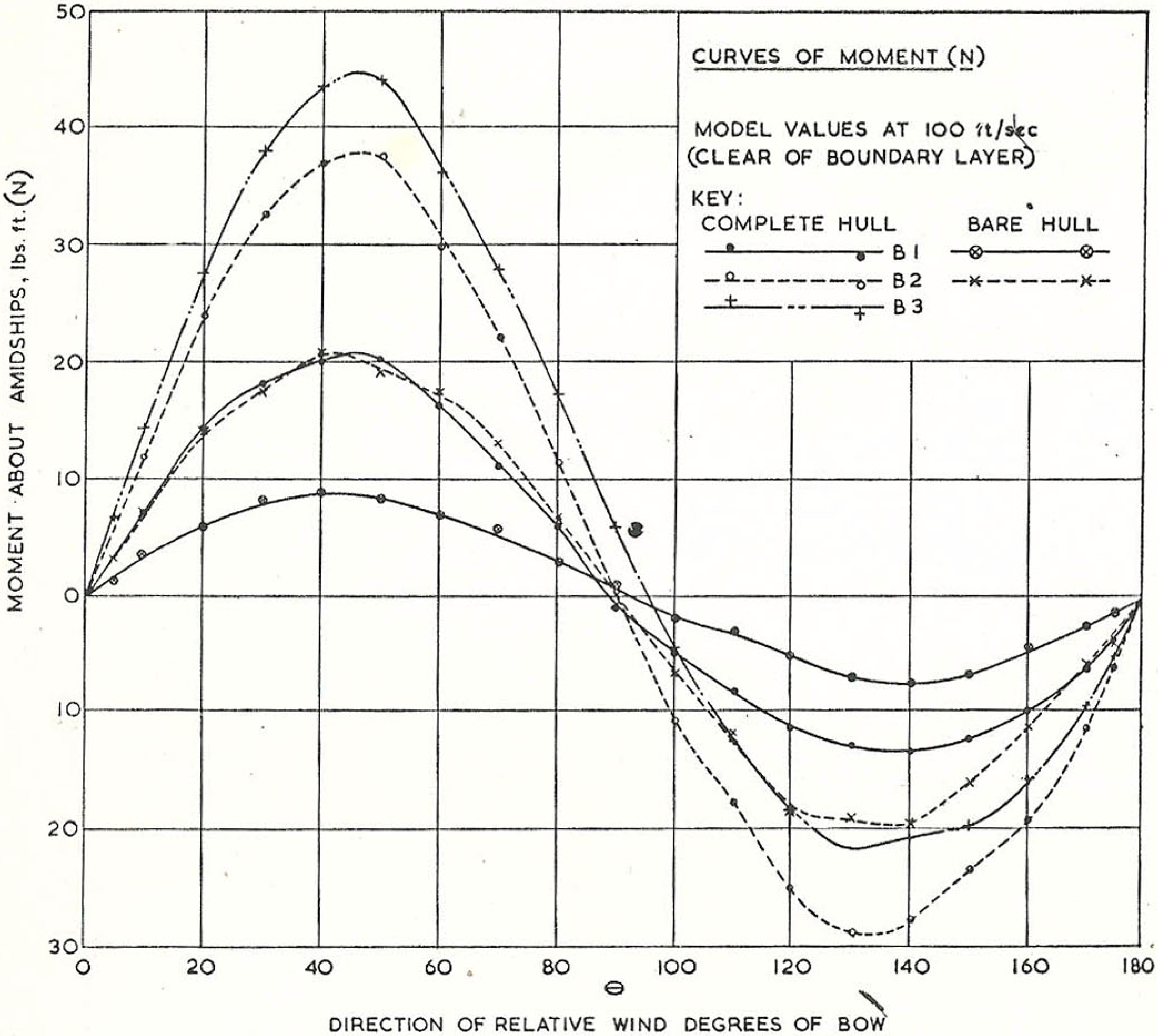

Fig. 10—*Cargo "B"*

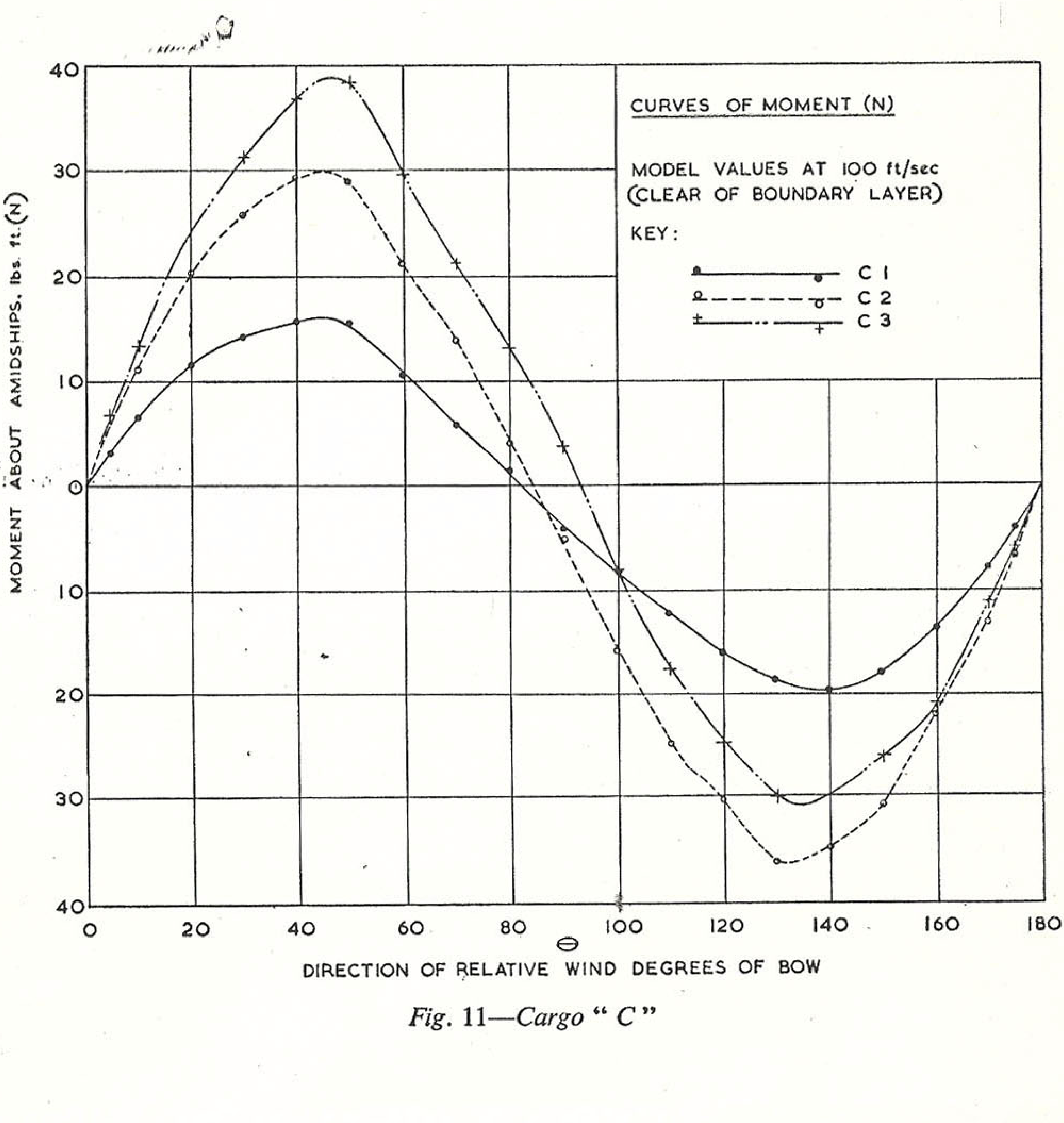

Fig. 11—*Cargo* " *C* "

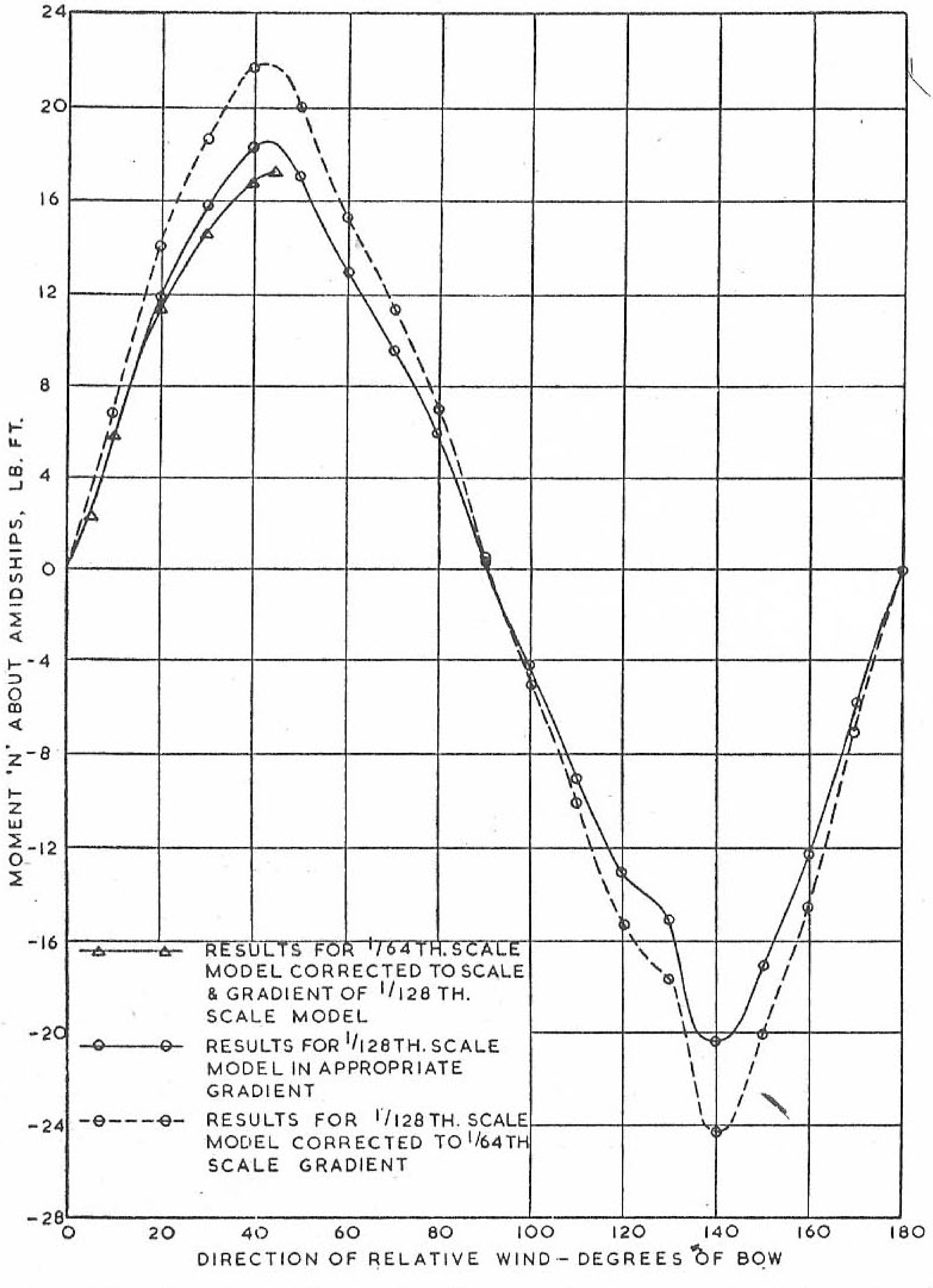

Fig. 12—Curves of Moments about Amidships for Model D (for Wind Gradient Condition and Wind Velocity of 100ft. per second)

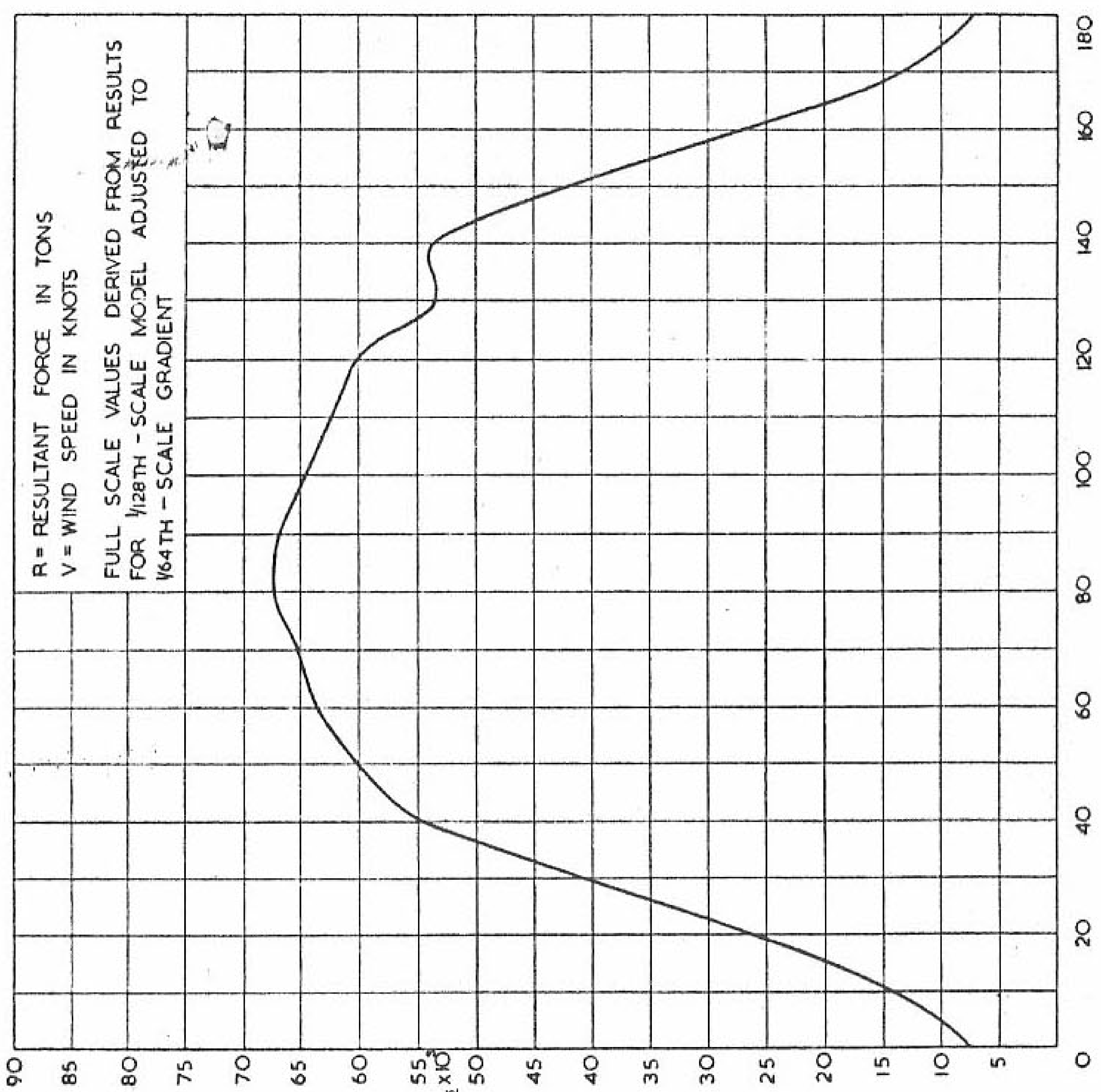

Fig. 14—Curve of $\frac{R}{V^2}$ *for Ship D (in Wind Gradient)*

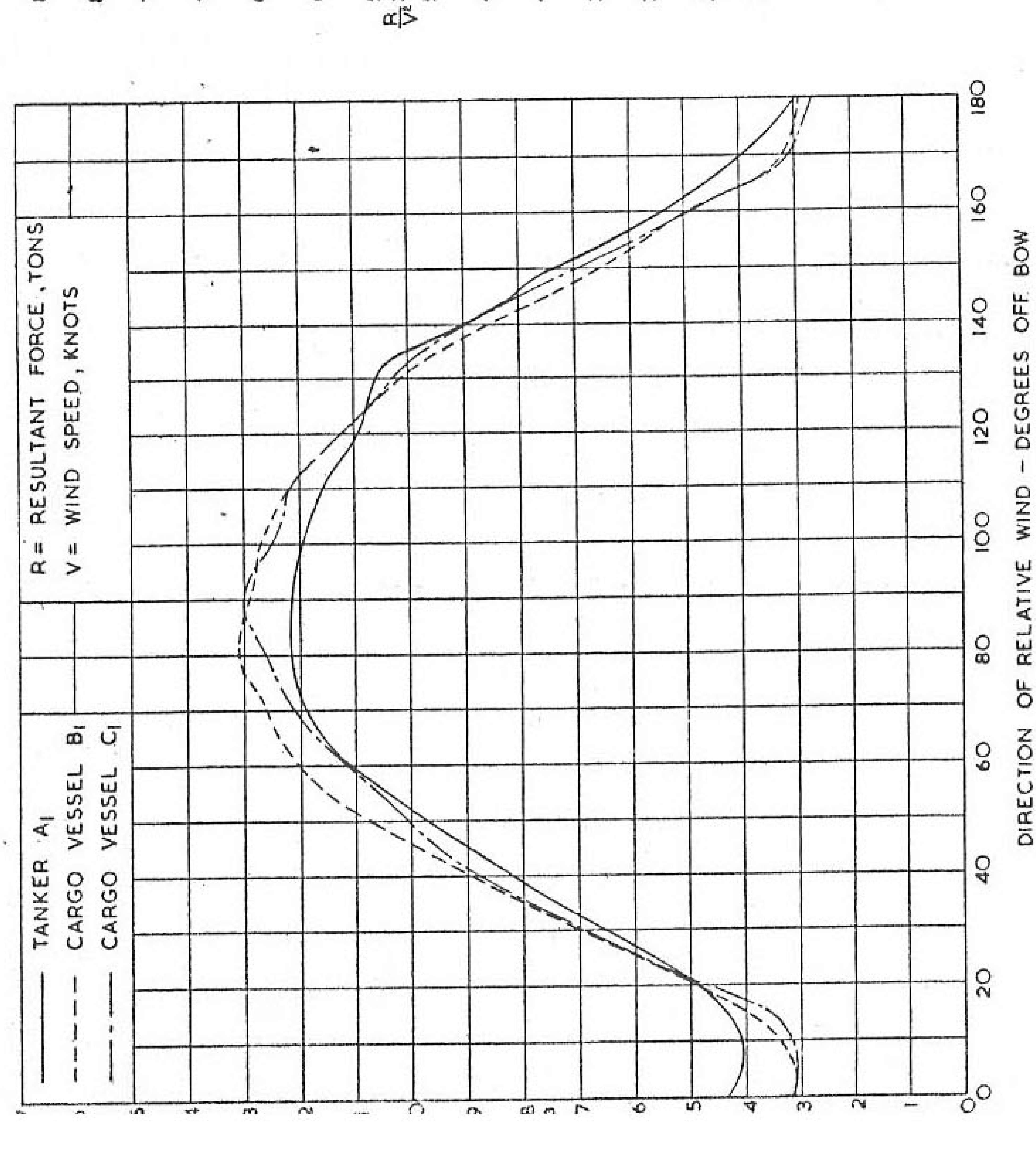

ig. 13—Curves $\frac{R}{V^2}$ *for Ships A1, B1 and C1 (in Wind Gradient)*

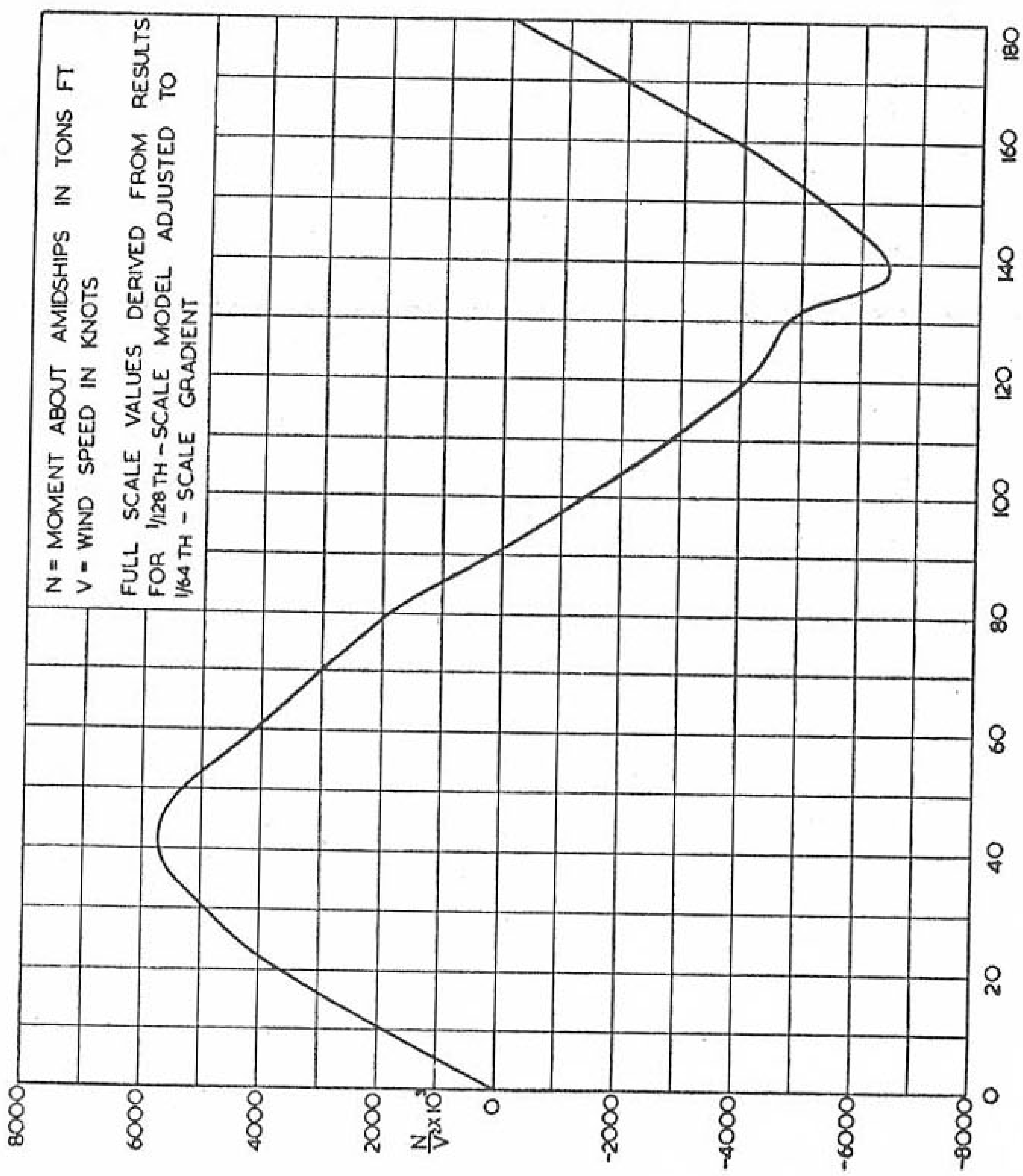

Fig. 16—*Curve of* $\frac{N}{V^2}$ *for Ship D (in Wind Gradient)*

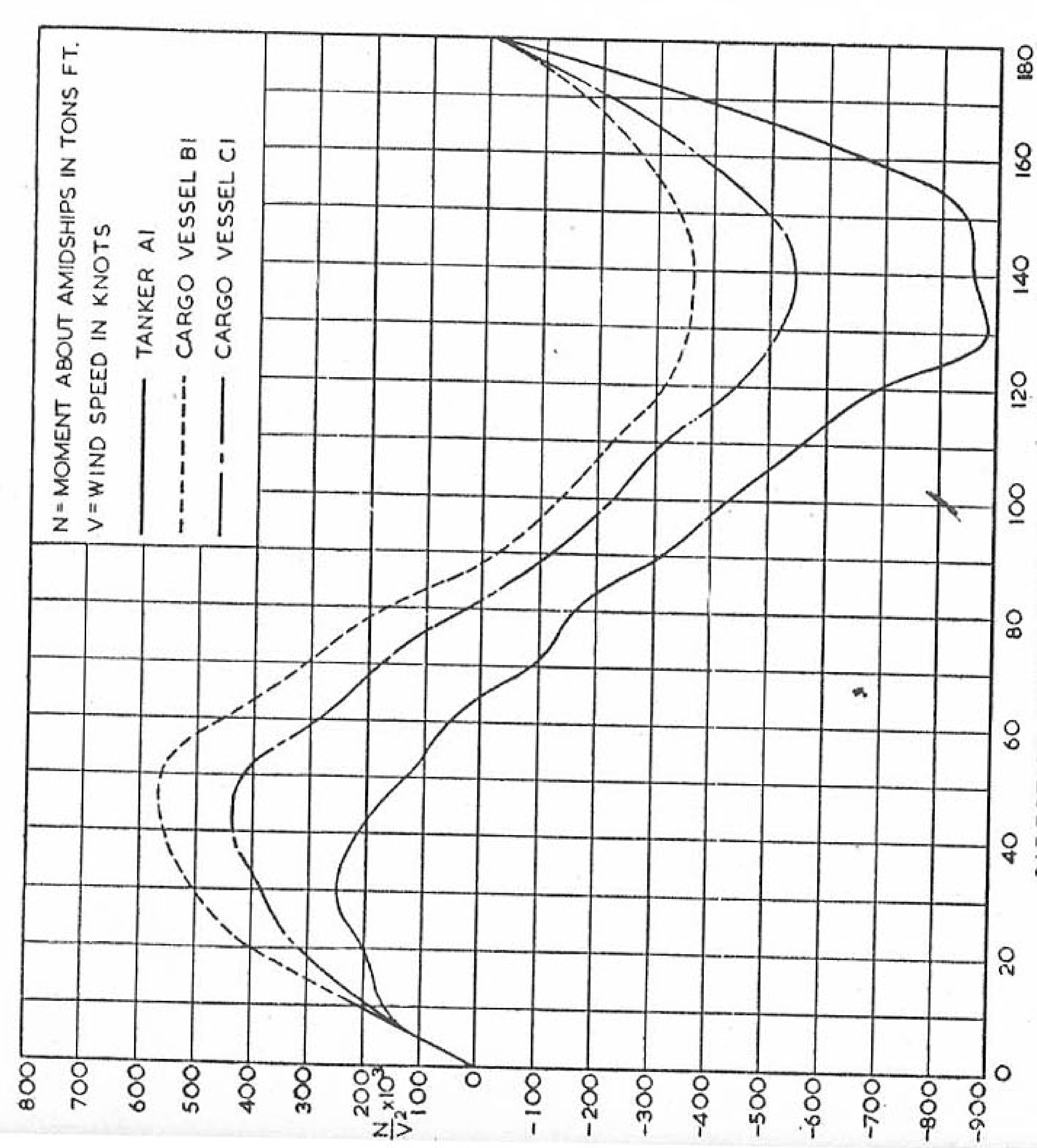

Fig. 15—*Curves of* $\frac{N}{V^2}$ *for Ships A1, B1 and C1 (in Wind Gradient)*

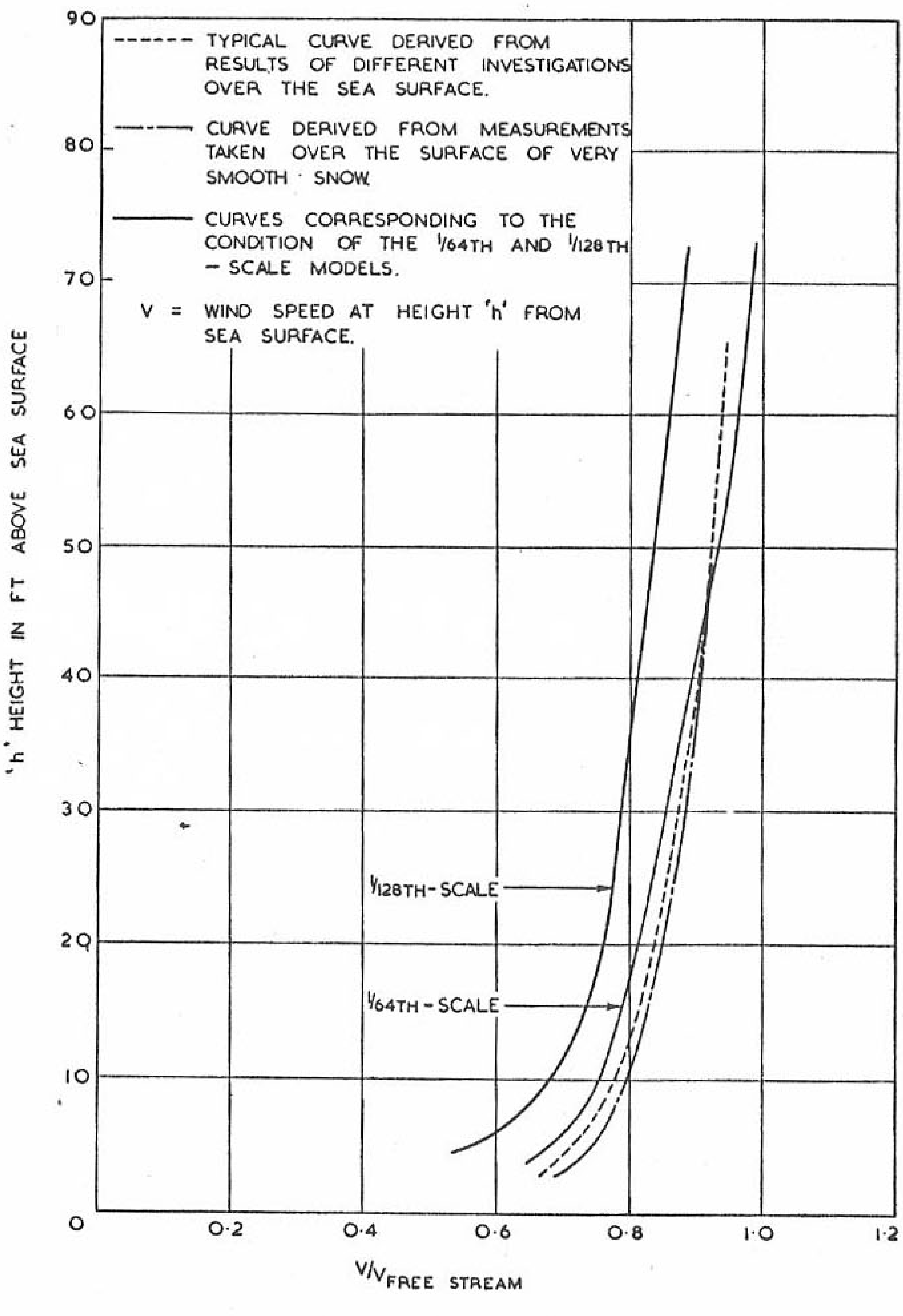

Fig. 17—*Velocity Gradients of Natural Winds compared with Tunnel Velocity Gradients adjusted to Full Scale*

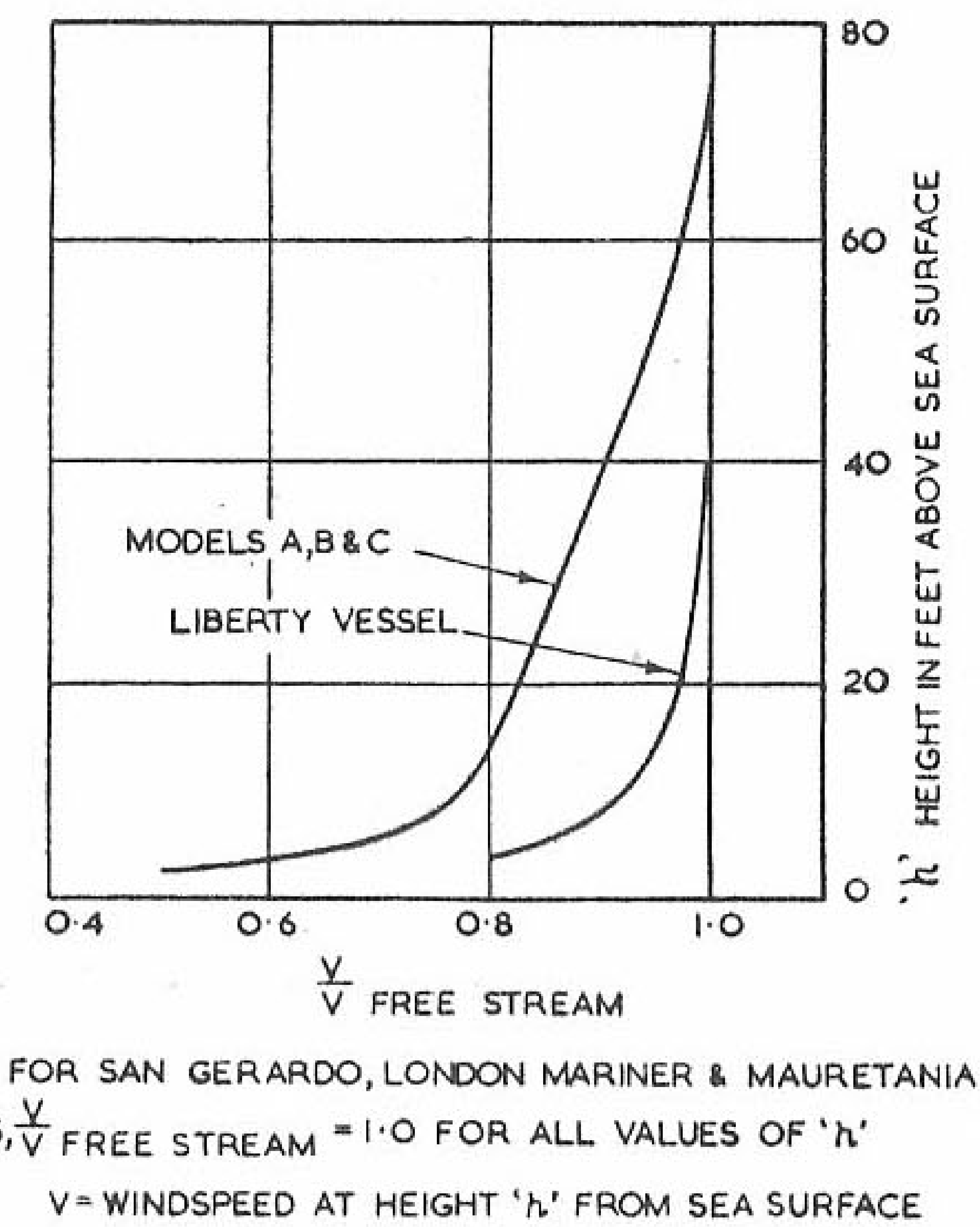

Fig. 18—Comparison of Wind Velocity Gradients. Models A B and C Tests and Liberty Vessel

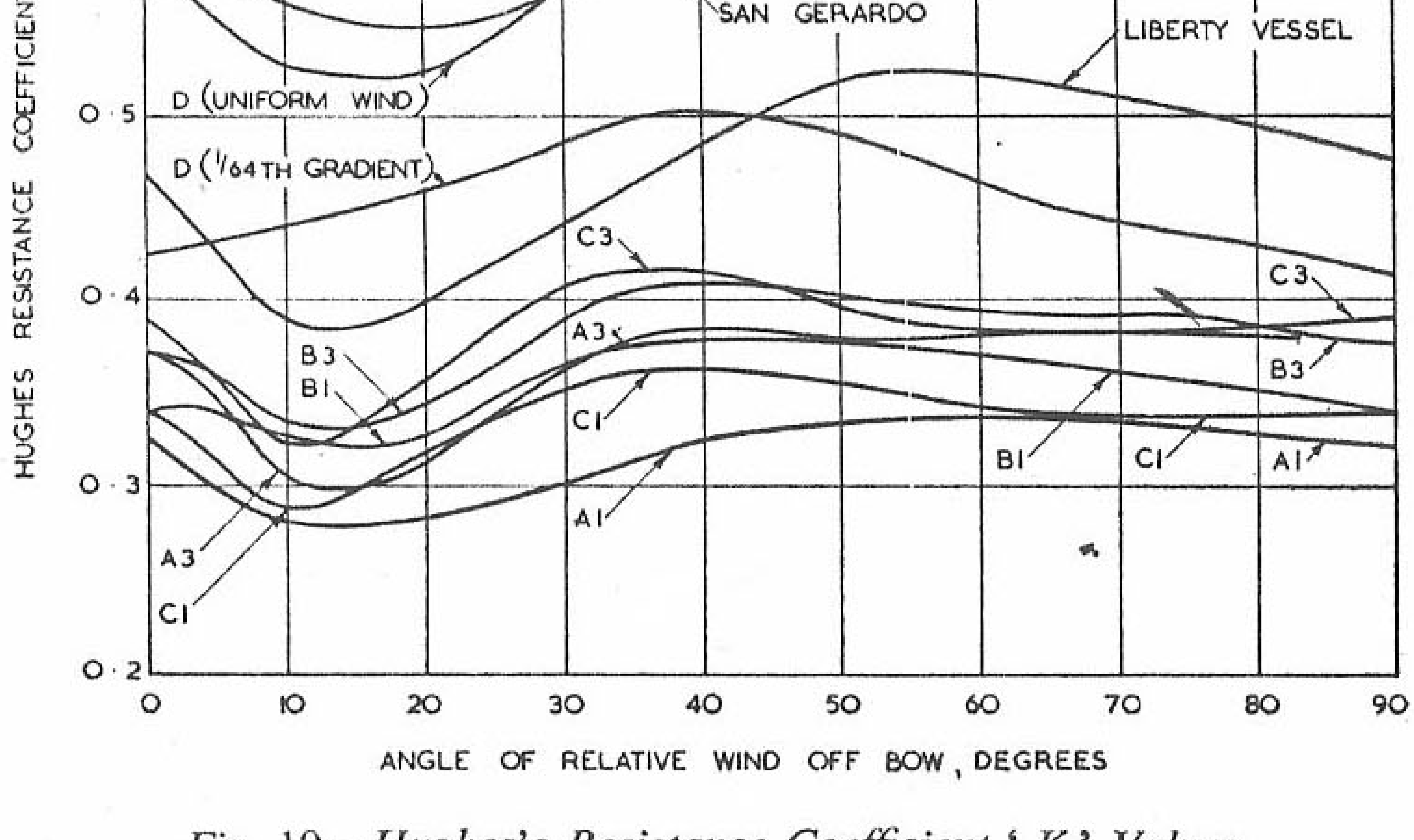

Fig. 19—Hughes's Resistance Coefficient 'K' Values

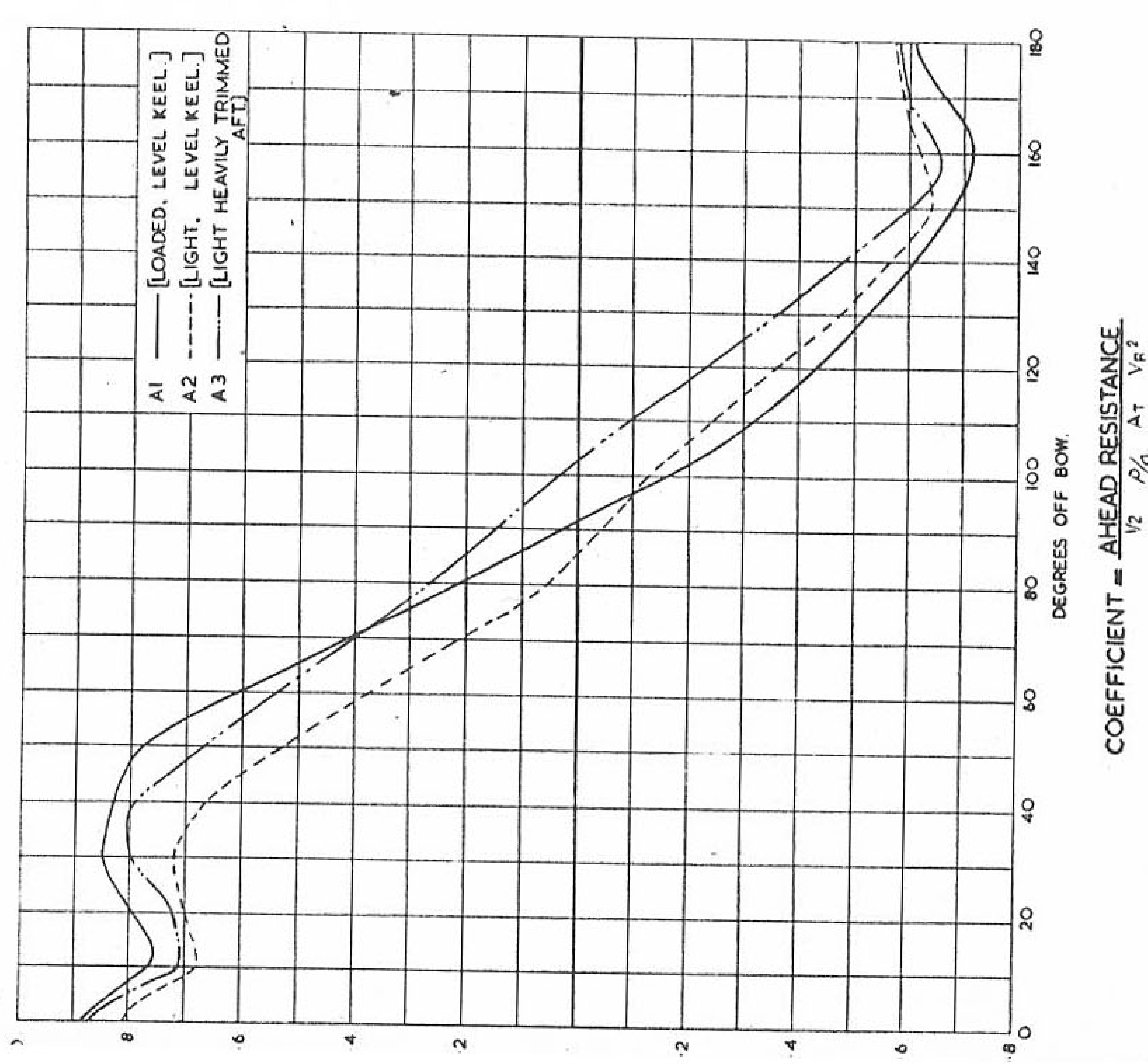

g. 20—Tanker "A" Curves of Ahead Resistance Coefficient in Three Conditions of Loading

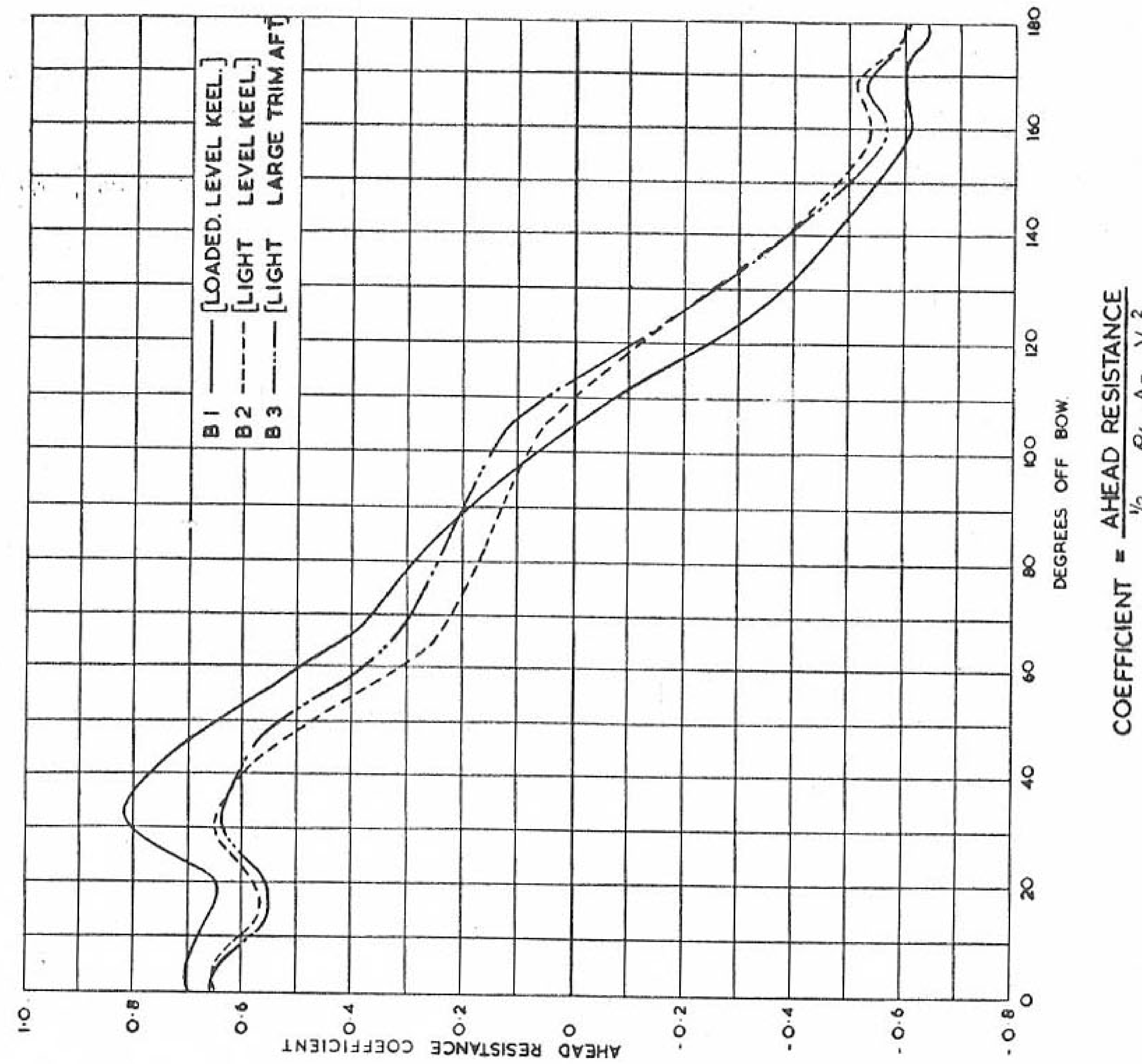

Fig. 21—Cargo "B" Curves of Ahead Resistance Coefficient in Three Conditions of Loading

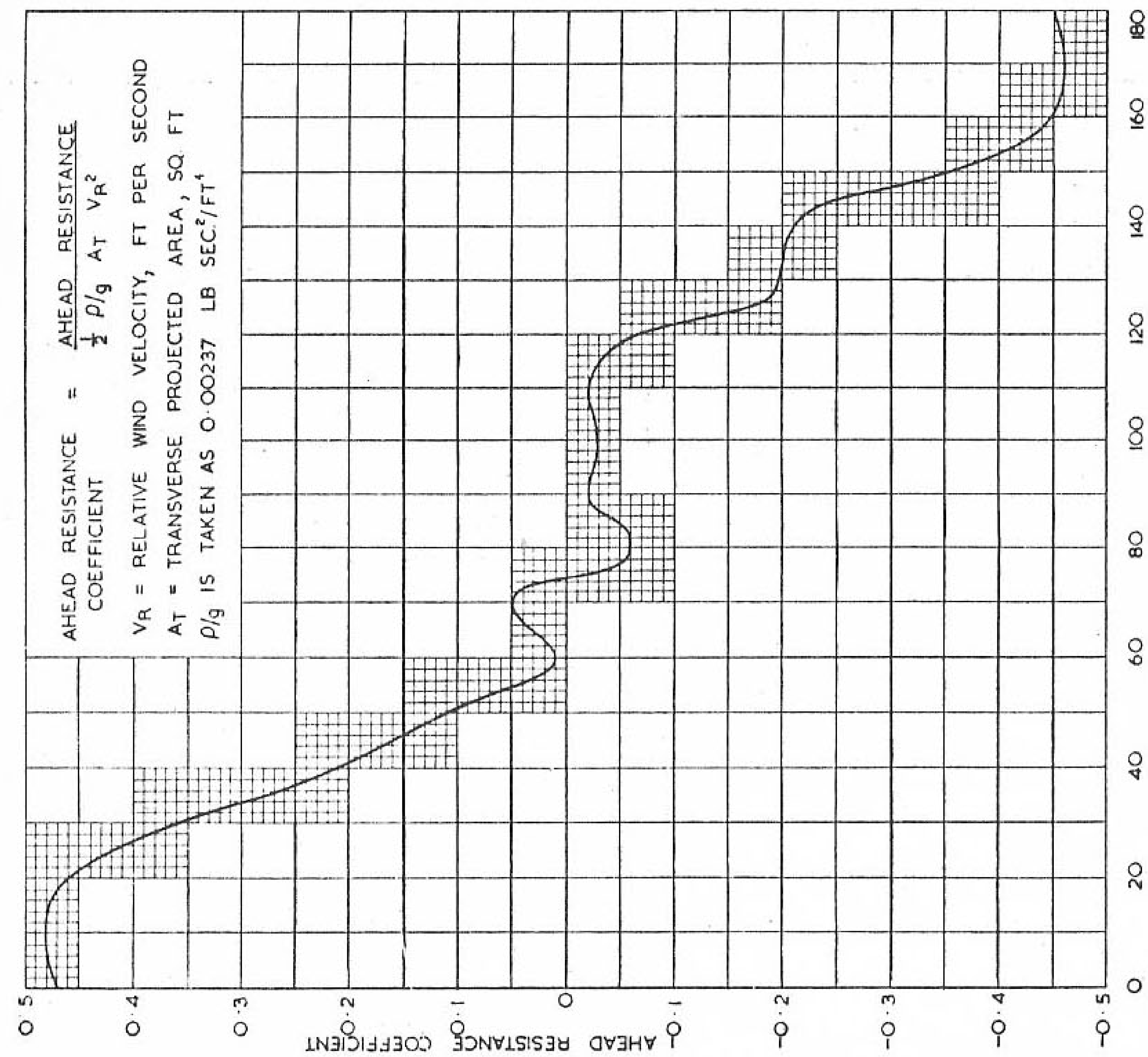

Fig. 23—Curve of Ahead Resistance Coefficient for Ship D (Derived from Results for 1/128th—Scale Model Adjusted to 1/64th-scale Gradient)

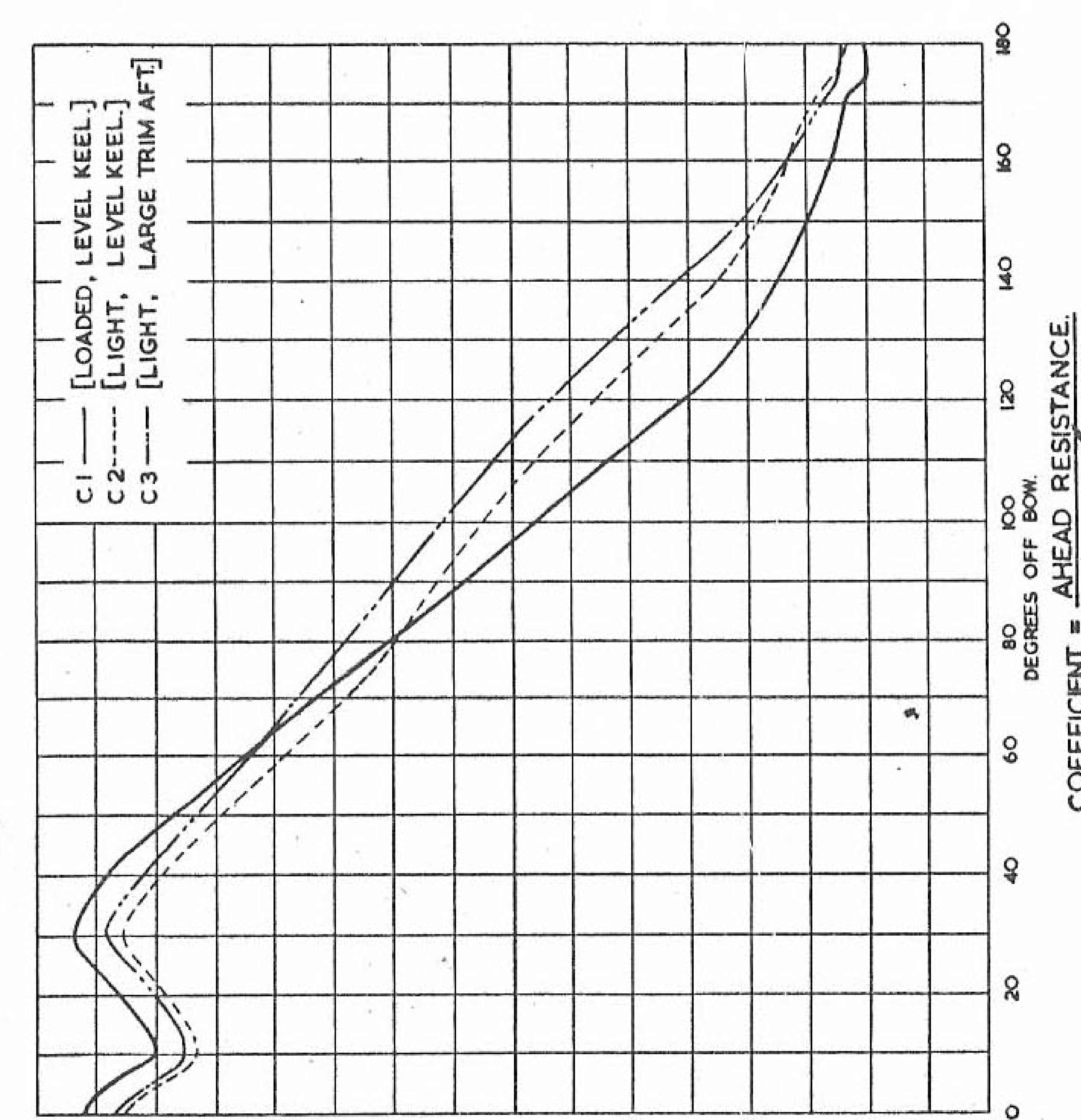

Fig. 22—Cargo " C" Curves of Ahead Resistance Coefficient in Three Conditions of Loading

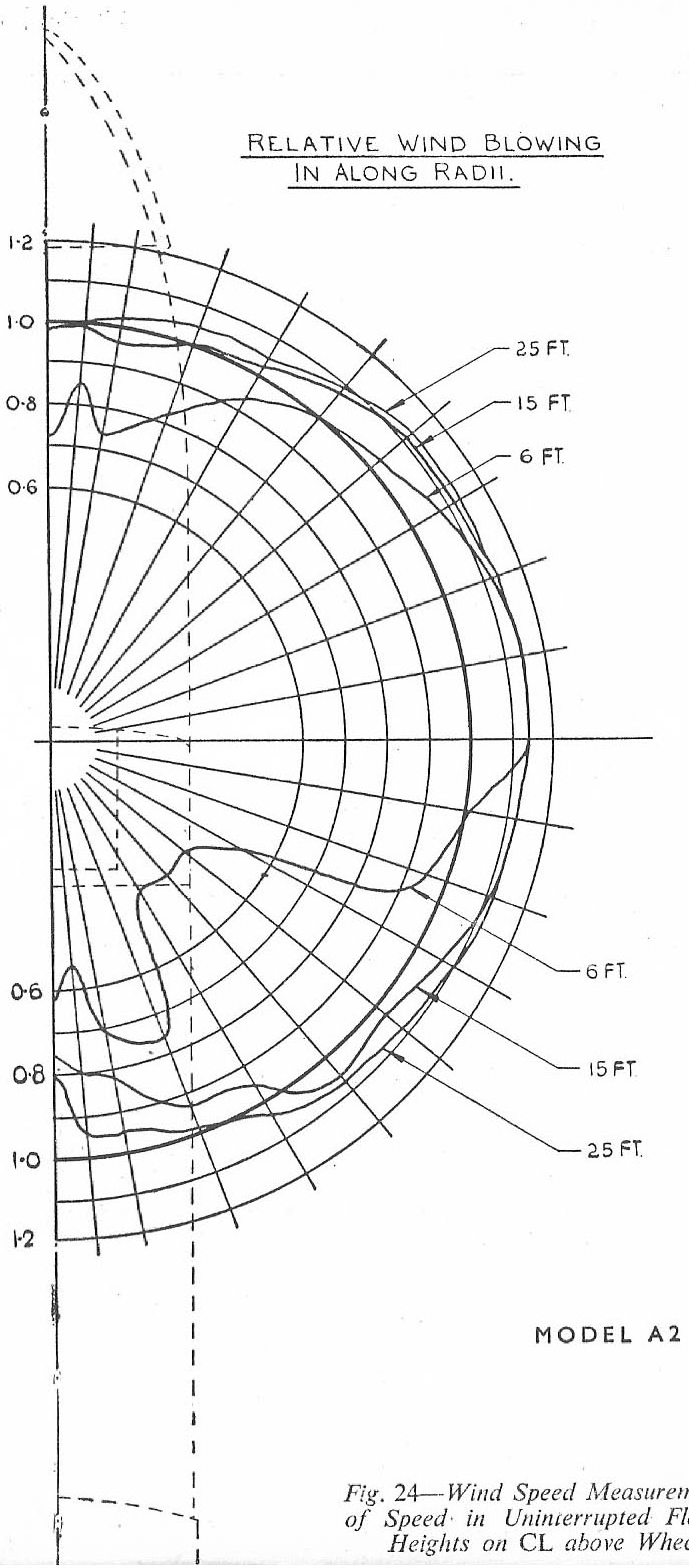

Fig. 24—Wind Speed Measurements as Ratios of Speed in Uninterrupted Flow. Various Heights on CL above Wheelhouse Top

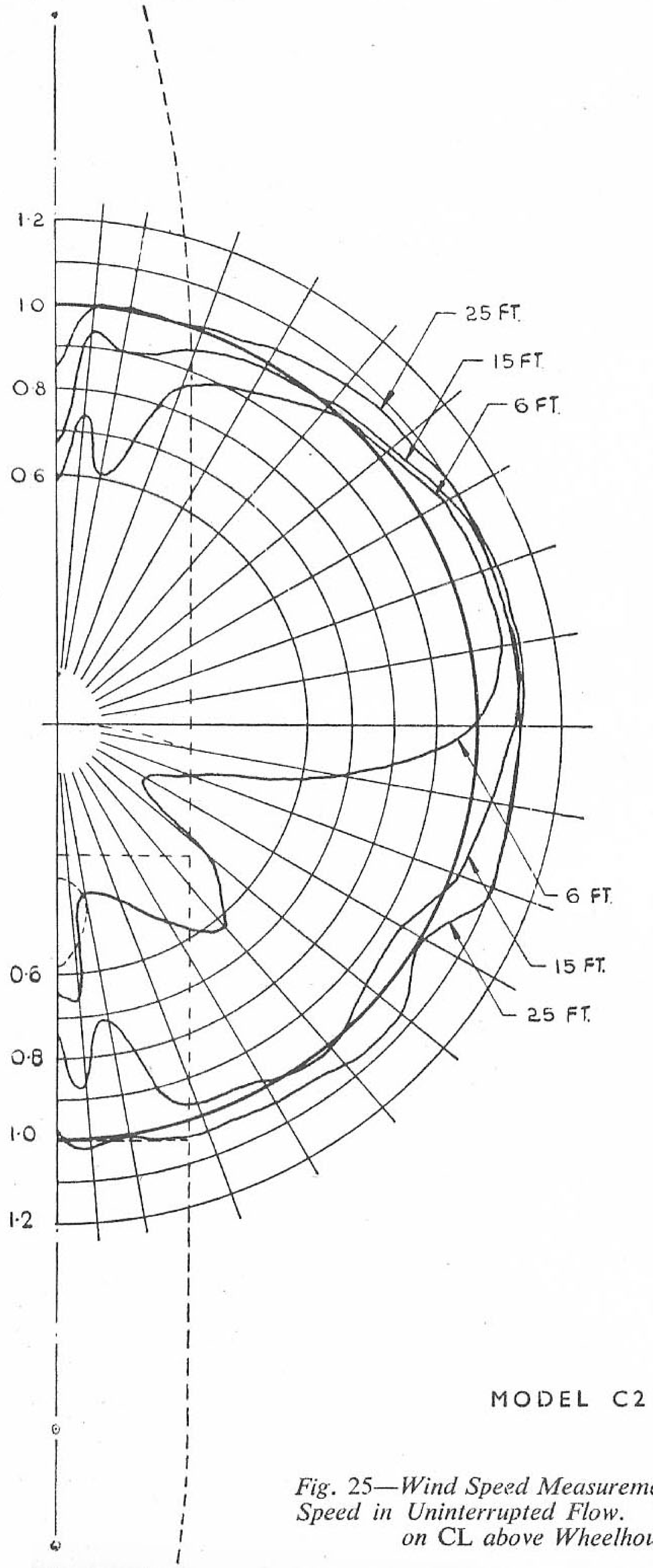

Fig. 25—Wind Speed Measurements as Ratios of Speed in Uninterrupted Flow. Various Heights on CL above Wheelhouse Top

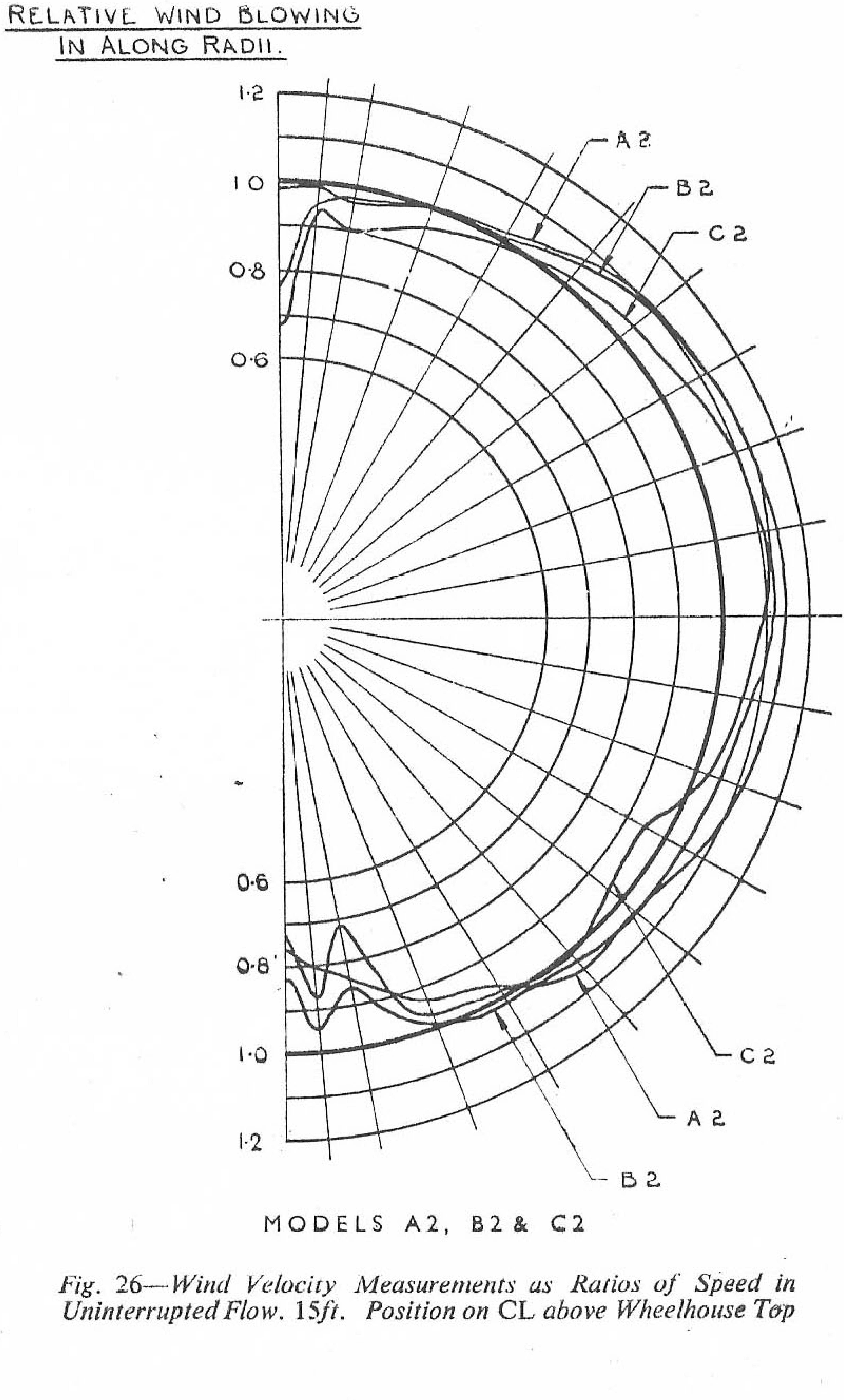

Fig. 26—Wind Velocity Measurements as Ratios of Speed in Uninterrupted Flow. 15ft. Position on CL above Wheelhouse Top

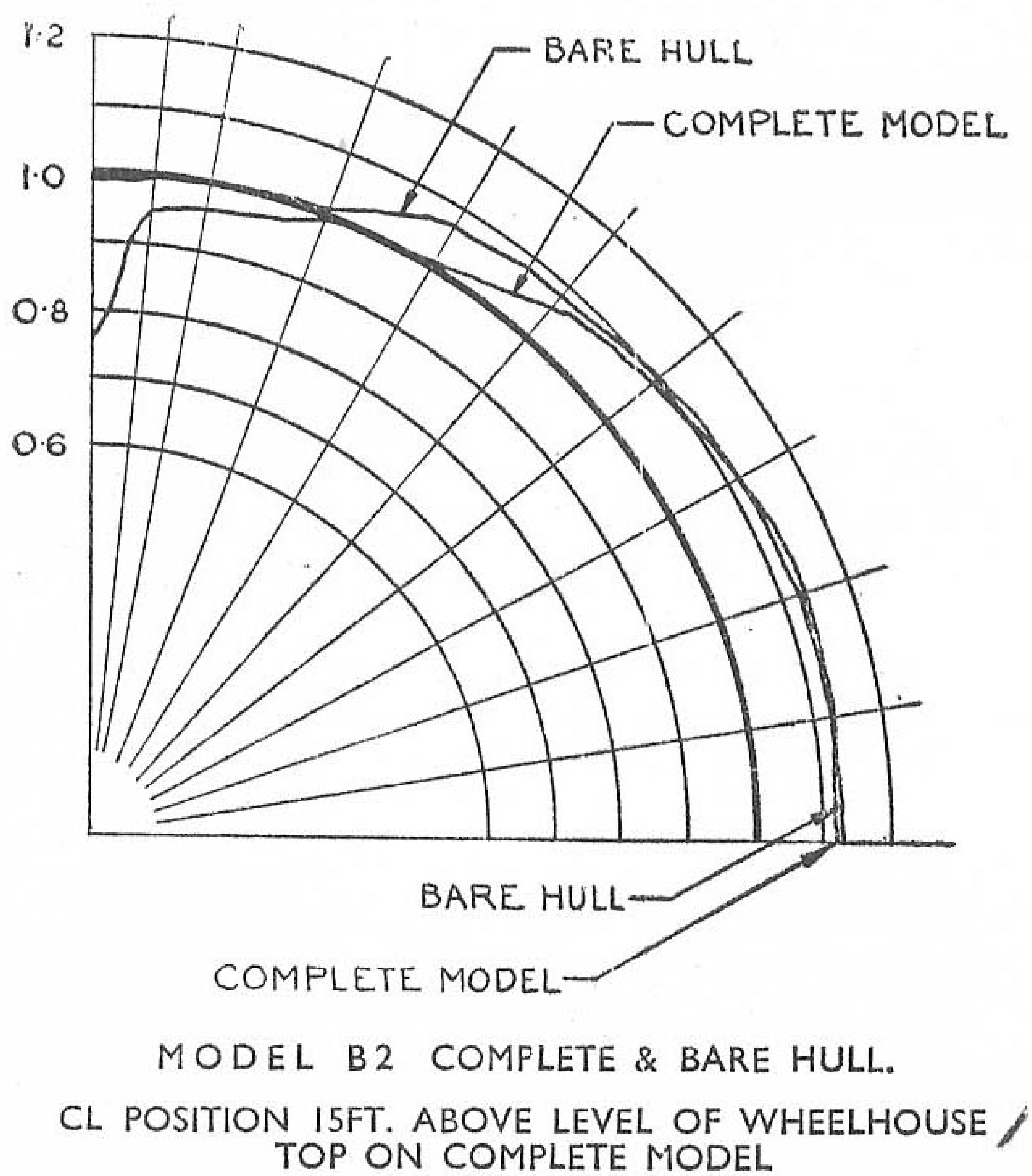

Fig. 27—Wind Velocity Measurements as Ratios of Speed in Uninterrupted Flow

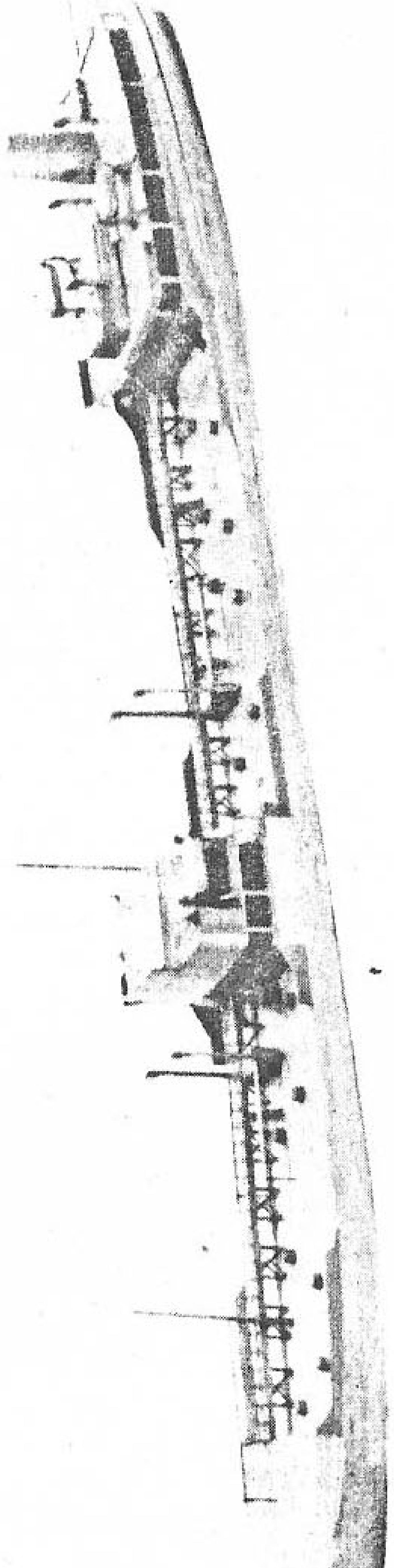

TANKER A

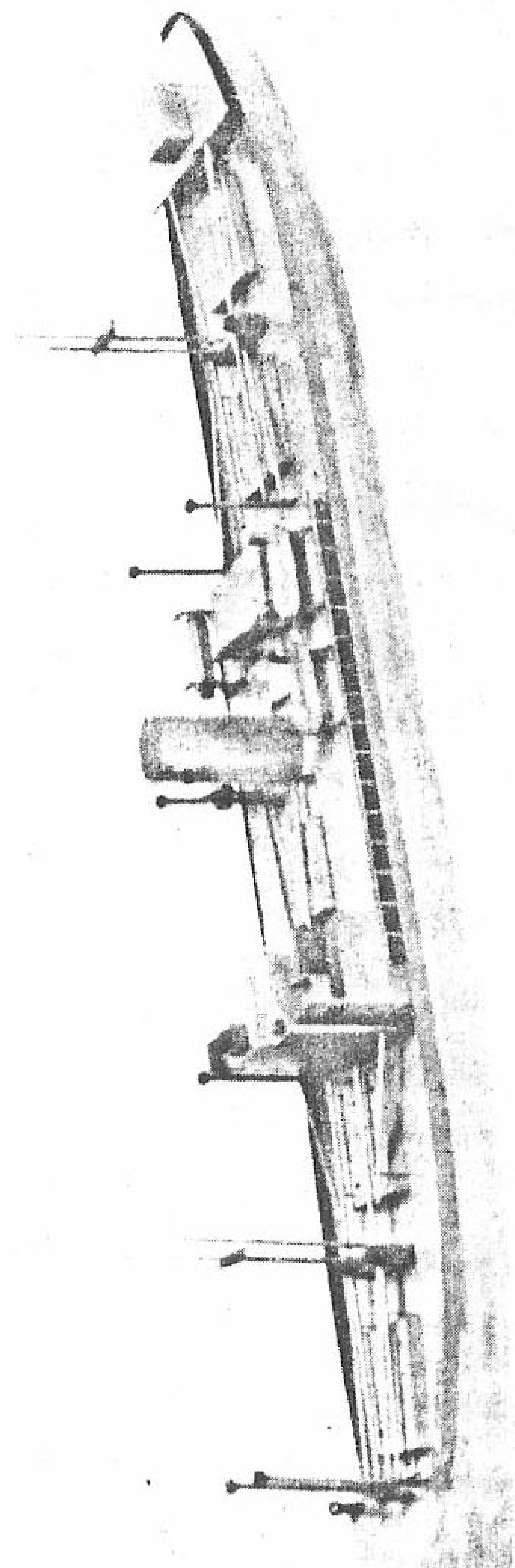

CARGO B

Fig.—28

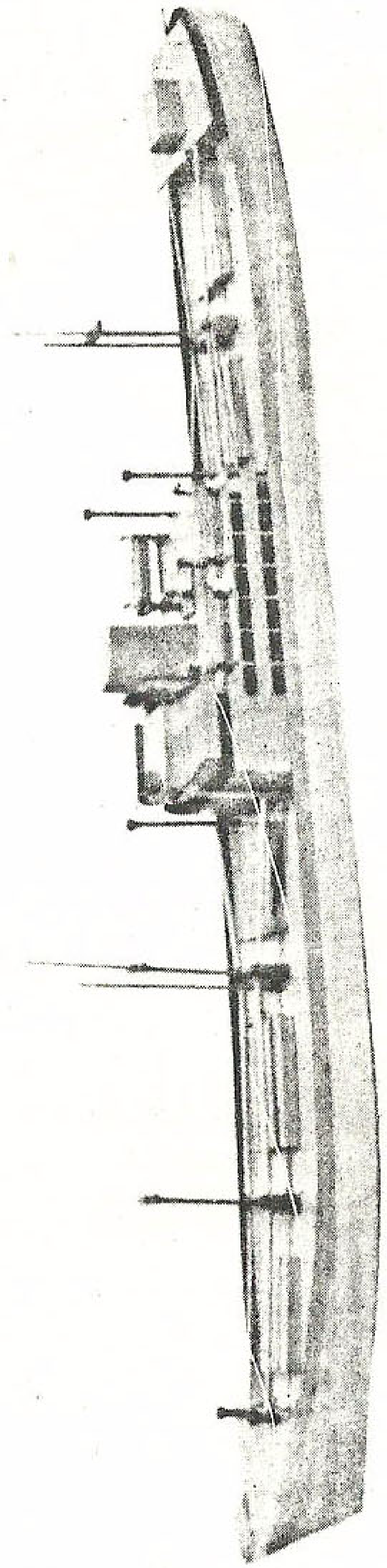

CARGO C

Fig. 28—*(continued)*

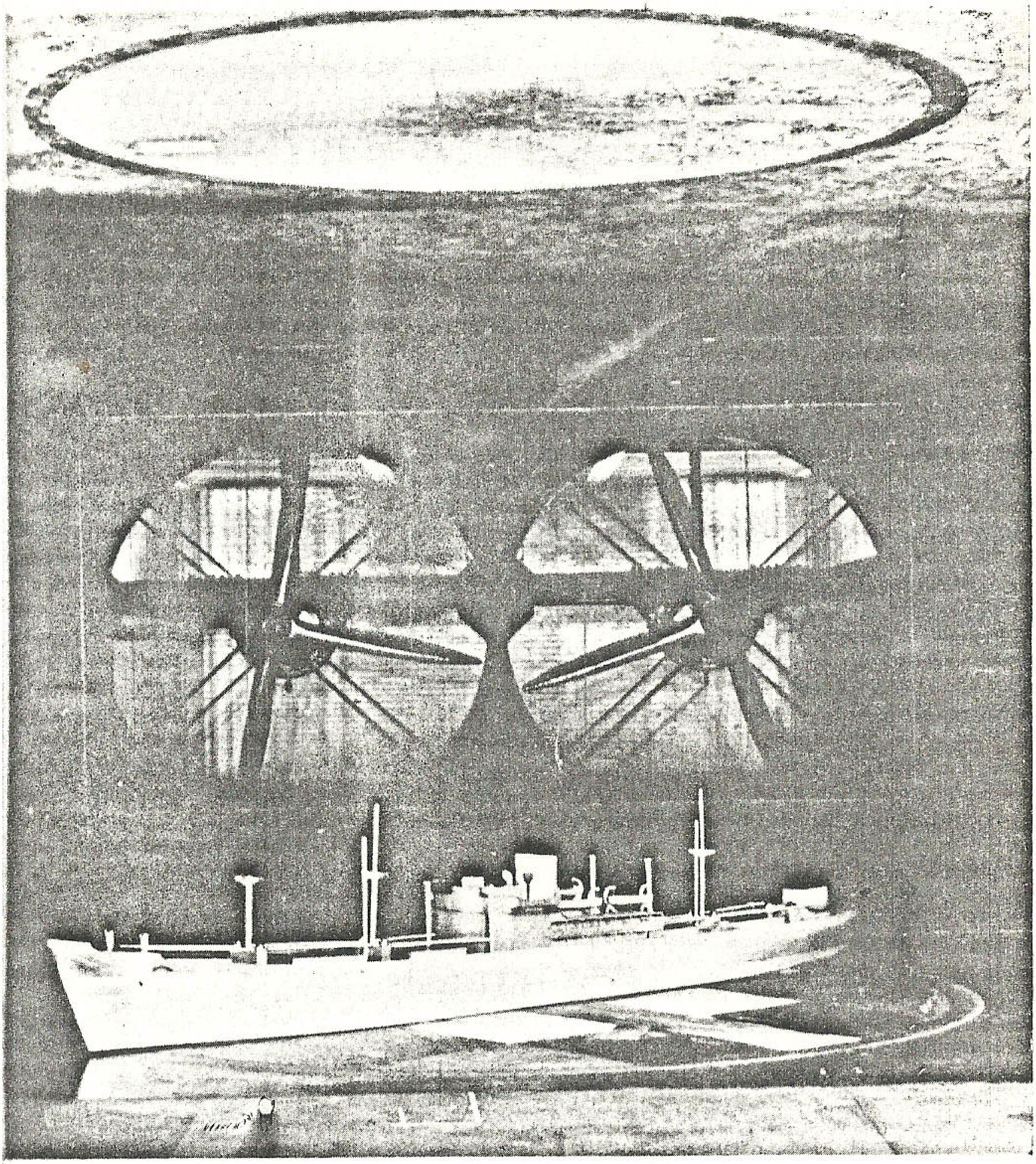

Fig. 29—Cargo " C " in Tunnel